IEEE Access
Multidisciplinary | Rapid Review | Open Access Journal

Received 24 March 2024, accepted 20 April 2024, date of publication 24 April 2024, date of current version 1 May 2024.

Digital Object Identifier 10.1109/ACCESS.2024.3392911

RESEARCH ARTICLE

Dynamic Multi-Objective Optimization of Grid-Connected Distributed Resources Along With Battery Energy Storage Management via Improved Bidirectional Coevolutionary Algorithm

ASIF ALI[1], ZHIZHEN LIU[1], AAMIR ALI[2], GHULAM ABBAS[3], EZZEDDINE TOUTI[4], AND WALEED NURELDEEN[5]

[1]School of Electrical Engineering, Shandong University, Jinan 250061, China
[2]Department of Electrical Engineering, Quaid-e-Awam University of Engineering Science and Technology, Nawabshah, Sindh 67450, Pakistan
[3]School of Electrical Engineering, Southeast University, Nanjing 210096, China
[4]Department of Electrical Engineering, College of Engineering, Northern Border University, Arar 73222, Saudi Arabia
[5]Department of General Subjects, College of Engineering, University of Business and Technology, Jeddah 23435, Saudi Arabia

Corresponding authors: Ezzeddine Touti (esseddine.touti@nbu.edu.sa) and Zhizhen Liu (liuzhizhen@sdu.edu.cn)

This work was supported by the Deanship of Scientific Research at Northern Border University, Arar, Saudia Arabia, under Project NBU-FFR-2024-2448-05.

ABSTRACT This paper explores the synergistic role of Distributed Resources (DR), including Distributed Generation (DG) and Battery Energy Storage Systems (BESS), in enhancing modern power systems' sustainability, reliability, and flexibility. It addresses the gap in concurrent distribution network reconfiguration and DR allocation, especially under the variability of renewable energy. The study aims to minimize energy costs, losses, and voltage deviations by integrating wind and solar PV-type DGs with BESS. A novel multi-objective function and an improved bi-directional coevolutionary (I-BiCo) Algorithm are employed to find the optimal RES and BESS placement and sizing, showing marked improvements over existing methods. Furthermore, statistical comparisons using hypervolume, objective function values (diversity), and near-global solutions (convergence) underscore the proposed algorithm's superiority over existing MOEAs. The final non-dominated solution, obtained through fuzzy set theory, highlights simulation results that minimize power loss, achieve substantial energy savings, and smooth demand, particularly with the integration of BESS devices. Moreover, optimal network reconfiguration (ONR) is a key strategy for balancing load demand. Simulation results affirm that minimizing bi-objective and tri-objective functions, coupled with optimal feeder reconfiguration, significantly reduces power loss and enhances voltage profiles, approaching unity across all buses. The proposed ONR formulation, in conjunction with DGs and BESS, maximizes the overall performance of power distribution networks. Furthermore, the paper addresses various time-dependent constraints of BESS, DG, and ONR, formulating and efficiently solving these constraints by integrating different constraint-handling techniques with the proposed multi-objective evolutionary algorithm. The study contributes to academic discourse and provides practical insights for designing more efficient and sustainable power systems in the face of evolving energy landscapes.

INDEX TERMS Distribution network, distributed generation, battery energy storage system, multi-objective evolutionary algorithm.

The associate editor coordinating the review of this manuscript and approving it for publication was Ilaria De Munari.

NOMENCLATURE

ABBREVIATIONS

DG	Distributed Generation.
PV	Photovoltaic.
WT	Wind Turbine.
SS	Sub-Station.
BESS	Battery Energy Storage System.
RES	Renewable Energy resource.
DR	Distributed Resources.
MOEAs	Multi-objective Evolutionary Algorithms.
BCS	Best Compromise Solution.
ONR	Optimal Network Reconfigurations.
I-BiCo	Improved Bidirectional Co-evolutionry.
GA	Genetic Algorithm.
NSGAII	Non-dominated Sorting Genetic Algorithms.
ND	Non-dominated.
AD	Angle-based Density.
CV	Constraint Violation.
VD	Voltage Deviation.
CEL	Cost of Energy loss.
PF	Pareto Front.
PS	Pareto Set.
HVI	Hyper Volume Indicator.
FR	Feasibility Ratio.
CDP	Constraint Domination Principle.
CMOP	Constrained Multi-objective Problem.

INDICES/ VARIABLES/ PARAMETERS

T_n	Span length of time.
N_DG	Total number of DGs.
nl	Total number of feeders.
N_b	Total number of buses.
$b \epsilon 1, .., N_b$	Index of a particular bus.
N_{BESS}	Total Number of BESS.
P_D,Q_D	Active and reactive load demand.
C_{SS},C_{DG},C_{BESS}	Cost of MW supplied by substation, DG, and BESS.
E_i^{min},E_i^{max}	Minimum and Maximum MWh capacity of BESS.
δ_{sr}	Voltage angle difference of branch between bus s and r.
$G_{(}(mn))$	Transfer conductance of branch between bus s and r.
$S_{(}lq)$	Actual MVA branch flow limit.
f_1	Cost of active power supplied by Grid Station.
f_2	Cost of Energy loss.
f_3	Voltage Deviation.
$\mathbf{x}$	Decision vector.
$h(\mathbf{x})$	Equality Constraint Function.
$g(\mathbf{x})$	Inequality Constraint Function.
$c_i(\vec{\mathbf{x}})$	ith degree of constraint Violation.
CV(x)	Overall Constraint Violation.
$C(P_g)$	Total operating cost of thermal generators.
p	Number of equality constraints.
p-q	Number of inequality constraints.
$site_{DG}$,$size_{DG}$	Optimal site and size of DG.
$site_{BESS}$,$size_{BESS}$	Optimal site and size of BESS.
$t \epsilon 1, \ldots, T_n$	Index of particular Time interval.
$i s \epsilon 1, \ldots, N_{DG}$	Index of generator.
$j \epsilon 1, \ldots, N_{BESS}$	Index of Particular BESS.
$l \epsilon 1, \ldots,$ nl	Index of Particular branch/feeder.
$m \epsilon 1, \ldots, N_L$	Index of Particular load bus.
P_{SS}, P_{DG}	Active power supplied by SS and DG.
P_{ch} and P_{dch}	Charging and discharging power of BESS.
N_L	Number of Load buses.
a	Direct cost parameter of SS.
k_1,k_2,k_3	Quadratic cost parameters of DG and BESS.
$C_{(P_{loss})}$, P_{loss}	Cost of active power loss and power loss in entire time span.
V_{SS}	Voltage set point at substation.
V_m	Voltage at mth load bus.
$SoC_(j(ini))$	Initial State of Charge.
Q_{loss}	Reactive Power loss.
Q_{SS},Q_{SS}^{min},Q_{SS}^{max}	Actual, minimum, and maximum MVAr of SS.
P_{SS},P_{SS}^{min},P_{SS}^{max}	Actual, minimum, and maximum MW of SS.
P_{DG},P_{DG}^{min},P_{DG}^{max}	Actual, minimum, and maximum MW of DG.
Q_{DG},Q_{DG}^{min},Q_{DG}^{max}	Actual, minimum, and maximum MVAr of DG.
V_{DG},V_{DG}^{min},V_{DG}^{max}	Actual, minimum, and maximum voltage set point of DG.
V_m,V_m^{min},V_m^{max}	Actual, minimum, and maximum voltage of load bus.
S_l, S_l^{max}	Actual and maximum MVA branch flow.
A	branch and bus incident matrix.
SoC	State of charge.

I. INTRODUCTION

A. LITERATURE REVIEW

According to [1], Distributed Resources (DR) of electric power are not directly connected to a bulk power transmission system. Distributed Resources (DR), including both Distributed Generation (DG) and Battery Energy Storage Systems (BESS), are integral components in the ongoing evolution of modern power systems. Their collective impact on sustainability, reliability, and flexibility aligns seamlessly with the broader objectives of transitioning towards cleaner and more resilient energy infrastructures. As technological advancements progress, the pivotal roles played by DG and BESS are expected to grow, contributing significantly to a more sustainable and adaptive energy landscape. While existing studies have individually focused on optimizing the integration of DG or network reconfiguration at a single

time, this paper addresses a critical gap by concurrently considering distribution network reconfiguration and DR allocation. Recognizing the challenges posed by the inherent variability of renewable energy sources, the paper introduces BESS to mitigate the limitations of multiperiod uncertain wind and solar PV integration. In this comprehensive study, wind and solar PV-type DGs, along with BESS, are utilized simultaneously to minimize the cost of energy supplied by the grid station, cost of energy loss, and voltage deviations in distribution networks. The optimal site and size determination of Renewable Energy Sources (RES) and BESS devices is achieved by formulating a new multi-objective objective function. An improved I-BiCo multi-objective Evolutionary Algorithm (EA) efficiently solves the proposed formulation, demonstrating superior convergence, diversity, and near-global solution identification compared to state-of-the-art MOEAs. The ONR's primary objective is to reduce active power losses in the distribution networks [2]. ONR is a mixed integer problem that is multi-objective and constrained non-linear [3], [4]. In addition to the advantages of introducing DGs into the power system, network reconfiguration is often witnessed as an additional approach to decrease losses in the distribution network. An ideal network configuration fulfills its operational needs while optimizing multiple variables, which can be achieved by managing the open/close status of sectionalizing and tie-switches throughout the optimal network reconfiguration process. Authors in [5] conducted the first network reconfiguration successfully to decrease active power losses. Multiple research studies have been undertaken in recent decades to address the network reconfiguration problem by incorporating extra parameters for optimization, which include voltage profile, system reliability indices, etc. Numerous optimization techniques, including genetic algorithms [6], modified honey bee mating optimization [7], binary group search [8], shuffled frog leaping algorithm [9], NSGAII [10], and artificial immune systems [11], are employed to perform distribution network reconfiguration to solve the multi-objective problems.

Due to the increasing demand for electricity and alarmingly rapid fossil fuel depletion, alternative energy sources have gained enormous attention during the past decade. As a result, research into integrating distributed generations (DGs) into distribution networks has received extensive emphasis [12]. Furthermore, placing a DG in the best locations with suitable size can mitigate the necessity of reactive power, improve the voltage profile, and reduce active power loss and line loading. Numerous researchers have suggested multiple optimization strategies to solve the formulated problem, which include conventional, artificial intelligence, and hybrid intelligent system techniques to solve the optimization problems [13]. Already carried out studies on the optimal DGs' integration in the distribution networks have only focused on the minimization of power loss and treated as a single objective function employing analytical approaches given in [14] and [15], heuristic and meta-heuristic methods which consist of genetic algorithm [8], ant lion optimization algorithm [16], and mixed integer non-linear programming [17]. The recent research brings out further objective functions to optimize DG siting and sizing, including higher voltage stability and reduced operational and carbon dioxide emissions costs. Genetic algorithm-based methods BSOA [18] and GA [19], computational methods ICA [20], MNLP [21], and ALOA [17], and hybrid optimization methods Fuzzy [22], and HPSO [14] are employed to achieve the expected results. However, these approaches suffer a lot from optimizing multiple objective functions simultaneously. Using weighted aggregation also makes the objective functions consume a long time to solve and find the desired solutions. In the second scenario, Pareto optimality is implemented to solve the optimization problems with various objective functions. Given that the multiple objective functions are optimized uniformly, the Pareto optimality technique yields Pareto sets of the best solutions to achieve optimal results. However, the primary method only produces a single outcome whenever each objective's value is selected. Recent studies have exploited multi-objective evolutionary algorithms based on the Pareto optimality concept to find the optimal locations and sizing of DGs, which comprises NSGAII [23], INSGAII [24], IMOHS [25], MOShBAT [26], and non-dominated sorting stochastic fractal search (NSSFS) [27], in an attempt to avoid this limitation. These evolutionary algorithms render a selection of Pareto-optimal solutions from which the network can make a fair decision. The distribution network reconfiguration and DGs' integration are typically analyzed individually. Nevertheless, combining these two sub-problems will be a better choice for the whole power system. There isn't enough literature that addresses network reconfiguration along with optimal DG allocation and sizing. The majority of the authors regard a single objective function to minimize power loss in the distributed networks. Researchers in [28], [29], [30], [31], [32], and [33] point out that comparatively a lesser amount of power was lost when the DG reconfiguration and integration were combined and optimized together to find the optimal solution. Only a few researchers have attempted to optimize this complex problem with extra objectives. In [34], the authors employed fuzzy-ACO (ant colony optimization) based on Pareto optimality to minimize active power loss, increase feeder loading balance balancing, and improve the voltage profile of the system. One DG on the PV array and DSTATCOM were employed to determine their optimal locations and sizes. Reference [35] used the multi-objective bang-big crunch technique to calculate the size of DGs without considering their optimal location. IPSO was used to solve the multi-objective problem of the coupled reconfiguration and optimal DGs integration [36]. Since these approaches assessed the weighted sum of the objective functions, Pareto optimality did not optimize the objectives evenly. Previously discussed research considered the models of DGs to be deterministic, while practically, they are

TABLE 1. Comparison of the proposed model with the most relevant studies.

Ref/Year/Method	S/M	DR Type							ONR	t_1	t_n	D/P	OF
		Non-Dispatchable			Dispatchable			B_{ESS}					
		P	Q	PQ	P	Q	PQ						
2018/SPEA2/[2]	☒/☑	☑	☒	☒	☒	☒	☒	☒	☑	☑	☑	☒/☑	PL, C, E
2022/BONMIN/[37]	☑/☒	☑	☒	☒	☒	☒	☒	☒	☒	☑	☒	☑/☒	PL
2022/IBPSO/[38]	☑/☒	☑	☒	☑	☒	☒	☒	☒	☒	☑	☒	☑/☒	C, CEL
2020/GWO/[39]	☑/☒	☑	☒	☑	☒	☒	☒	☒	☒	☑	☒	☑/☒	PL
2020/EAEO/[40]	☑/☒	☑	☒	☑	☒	☒	☒	☒	☒	☑	☒	☑/☒	PL, VD, SI
2020/EGA/[41]	☑/☒	☑	☒	☑	☒	☒	☒	☒	☒	☑	☒	☑/☒	PL,QL,VD
2022/JSA/[42]	☑/☑	☑	☒	☑	☑	☑	☑	☒	☒	☑	☒	☑/☒	C, PL, QL, VD, SI
2020/Cf-PSO/ [43]	☑/☑	☑	☒	☑	☒	☒	☒	☒	☒	☑	☒	☑/☒	C, PL, QL, VD, SI
2022/GWO/[44]	☑/☑	☑	☒	☑	☒	☒	☒	☒	☒	☑	☒	☑/☒	PL, QL, VD, SI
2020/DE/[45]	☒/☑	☑	☒	☑	☒	☒	☒	☑	☒	☒	☑	☑/☒	VD, PL, I_3
2021/ EGWO-PSO/[46]	☑/☑	☑	☒	☑	☒	☒	☒	☒	☒	☑	☒	☑/☒	C, E, PL, VD
2018/ALO/[47]	☑/☑	☑	☒	☒	☒	☒	☒	☒	☒	☑	☒	☑/☒	C, PL, VD
2020/PSO/[48]	☑/☒	☑	☒	☒	☒	☒	☒	☑	☑	☒	☑	☑/☒	PL, VD
2018/WCA/[49]	☑/☒	☑	☑	☒	☒	☒	☒	☒	☒	☑	☒	☑/☒	C, PL, VD, SI
2020/MRFO/[50]	☒/☑	☑	☒	☑	☒	☒	☒	☒	☒	☑	☒	☑/☒	PL, VD, SI
2021/WOA/[51]	☒/☑	☑	☒	☑	☒	☒	☒	☒	☒	☑	☑	☑/☒	PL,VD
2015/ACO-ABC/[52]	☑/☑	☑	☒	☑	☒	☒	☒	☒	☒	☑	☒	☑/☑	C,E,PL,SI
2018/MINLI-ECM/[53]	☒/☑	☑	☒	☑	☒	☒	☒	☒	☒	☑	☑	☑/☒	C, E
2020/GA-DE-SPEA2/[54]	☒/☑	☑	☒	☒	☒	☒	☒	☒	☒	☒	☑	☒/☑	C, E, SI
2022/MSLF/[55]	☑/☑	☑	☒	☒	☒	☒	☒	☒	☒	☒	☑	☑/☒	C, CEL, PL
2022/MALO/[56]	☑/☑	☑	☑	☒	☒	☒	☒	☒	☒	☑	☒	☑/☒	PL, QL,VD,SI
2019/MOCMIEP/[57]	☒/☑	☑	☑	☒	☒	☒	☒	☒	☒	☑	☒	☑/☒	PL, SI, E
2022/IGWOPSO/[58]	☒/☑	☑	☑	☒	☒	☒	☒	☒	☒	☑	☒	☑/☒	PL,VD,SI
2021/MOMVO/[59]	☒/☑	☑	☑	☒	☒	☒	☒	☑	☒	☒	☑	☑/☒	C,VD
2017/MOEAD/[60]	☒/☑	☑	☑	☒	☒	☒	☒	☒	☒	☑	☒	☑/☒	PL, QL
2021/I-DBEA/[61]	☒/☑	☑	☑	☒	☒	☒	☒	☒	☒	☑	☒	☑/☒	PL,SI,VD
2020/CSSA/[62]	☒/☑	☑	☑	☒	☒	☒	☒	☑	☒	☒	☑	☑/☒	PL, SI, VD
Proposed	☑/☑	☑	☑	☑	☑	☑	☑	☑	☑	☑	☑	☑/☑	C, CEL, VD

S: Single objective; M: Multi-objective; DR: Distributed Resources; B_{ESS}: Battery Energy Storage System; ONR: Optimal Network Reconfiguration; t_1: Single Period; t_n: Multi-period; D: Deterministic; P: Probabilistic

intermittent in nature, especially renewable energy-based DGs. Most of the authors in the studied literature have focused on the optimal placement of distributed generations (DGs) and reconfiguration for a single period only. Several other studies on distribution network enhancement have focused on optimizing distributed generations (DG) integration or network reconfiguration only. However, limited research has been conducted on the distribution network reconfiguration and the DG allocation simultaneously. Renewable DGs allocations in distribution are especially crucial due to environmentally friendly sustainability, such as no GHG, independent of fuel, reduced losses, and economic growth. Their importance continues to grow as societies and utilities strive to transition toward cleaner and more resilient energy systems. Still, it is highly uncertain, causing scheduling problems in the power system. The intermittency, variability, and mismatch between supply and demand are some issues associated with integrating renewable energy supplies into the grid. Systems for storing energy in batteries, or BESS, answer these issues.

B. CONTRIBUTION AND PAPER ORGANIZATION

Battery energy storage systems (BESS) are essential in managing and optimizing renewable energy utilization. They guarantee a steady and reliable power supply by accruing surplus energy throughout high generation and discharging it during demand. It diminishes power variations and keeps grid stability while plummeting the necessity for costly power sources. BESS helps the system through emergencies and variations by augmenting power quality and supplying auxiliary power. Via this action, the dependability and effectiveness of renewable energy are improved to promote further economical and durable energy future. The crux of the recent research work is thoroughly and comprehensively compared to the proposed algorithm in Table 1.

Table 1 shows that the proposed algorithm reveals an all-inclusive method by integrating multiple factors not jointly found in the above literature. This technique effectively combines distributed resources (DRs) that encompass distributed generation (DG) and battery energy storage systems (BESS) with the optimal network reconfiguration (ONR). This algorithm is multi-objective, which includes both single and multi-period scenarios. It also integrates deterministic and probabilistic techniques to find a robust solution. The proposed approach makes significant contributions, which consist of cost minimization (C), energy loss reduction (CEL), and voltage deviation (VD), which significantly outperforms numerous present methods. The proposed algorithm clearly shows substantial improvement in the multiple categories compared to other state-of-the-art algorithms, highlighting its effectiveness and superiority in optimizing distribution networks.

This study focuses on the importance of Renewable Distributed Generators (DGs) and Battery Energy Storage Systems (BESS) in improving distribution networks' environmental and economic characteristics. It solves the complex challenges posed by renewable energy sources, which are intermittent and variable, via dynamic multi-objective network reconfiguration of DGs and BESS. This paper introduces a novel multi-objective Improved Bi-directional coevolutionary algorithm (I-BiCo), which shows the enhancements in the solutions, validating its efficiency and robustness. This study substantially contributes by plummeting the cost of energy delivered, energy loss, and voltage variations. It also presents a complete approach by concurrently considering distribution network reconfiguration and optimal DG and BESS allocation, considering wind and solar power variability. The proposed algorithm optimizes the sitting and sizing of renewable energy sources and BESS devices, improves network reliability, manipulates energy storage, and exploits a multi-objective optimization framework. The algorithms are applied at a 72-hour time, incorporating natural load curves considering local climate data by finding a promising and holistic solution. This paper thoroughly validates its applicability against the other Multi-Objective Evolutionary Algorithms (MOEAs) and demonstrates its superior convergence, diversity, and solution quality performance. Its multi-dimensional optimization framework effectively balances the load demand by reducing power losses, improving voltage profiles, and significantly enhancing the performance and sustainability of power distribution networks.

The contributions of this work are as follows:

- ➢ Introducing a novel multi-objective Improved Bi-directional coevolutionary algorithm (I-BiCo) for dynamic optimization of distribution networks through the integration of Renewable Distributed Generators (DGs) and Battery Energy Storage Systems (BESS) along with optimal network reconfiguration.
- ➢ Enhancing environmental and economic performance of distribution networks by addressing the intermittent nature of renewable energy sources and optimizing network reconfiguration.
- ➢ Reducing costs, energy losses, and voltage deviations significantly, outperforming existing state-of-the-art algorithms in these domains.
- ➢ Optimizing the siting and sizing of renewable energy sources and BESS devices to improve network reliability, manage energy storage, and exploit a multi-objective optimization framework.
- ➢ Applying the algorithms over a 72-hour period to incorporate natural load curves and local climate data, offering a holistic solution approach.
- ➢ Demonstrating superior convergence, diversity, and solution quality performance compared to other Multi-Objective Evolutionary Algorithms (MOEAs), thereby significantly enhancing power distribution networks' performance and sustainability.

The rest of the paper is given as well. Section II presents the reconfiguration, DR sizing, and allocation mathematical formulation. Section III describes the I-BiCo Algorithm implementation for ONR and DR allocation. Section IV asylums time-varying device modeling and study cases. Section V covers Simulation Results Analysis and Scenario Comparison. Section VI concludes the paper.

II. MULTI-OBJECTIVE PROBLEM FORMULATION

This paper presents three objective functions to improve distribution system performance. The optimal integration and parallel reconfiguration of DGs serve to reduce the cost of energy supplied (C), cost of energy loss (CEL), and voltage variation (VD) by determining the optimal distribution network and DG locations and sizes. With the following mathematical formulation [63], this non-linear mixed integer non-linear problem is considered a multi-objective optimization (MOO) problem.

$$\begin{aligned} &\min \mathrm{F}\left(\vec{\mathbf{x}}\right) = \left(\mathrm{f}_1^{\mathrm{t}}\left(\vec{\mathbf{x}}\right), \mathrm{f}_2^{\mathrm{t}}\left(\vec{\mathbf{x}}\right), \ldots, \mathrm{f}_{\mathrm{m}}^{\mathrm{t}}\left(\vec{\mathbf{x}}\right)\right) \in \mathrm{R}^{\mathrm{m}} \\ &\text{s.t. } \mathrm{h}_{\mathrm{i}}^{\mathrm{t}}\left(\vec{\mathbf{x}}\right) = 0, \mathrm{i} = 1, \ldots, \mathrm{p} \\ &\quad \mathrm{g}_{\mathrm{i}}^{\mathrm{t}}\left(\vec{\mathbf{x}}\right) \leq 0, i = \mathrm{p}+1, \ldots, \mathrm{q} \\ &\quad \vec{\mathbf{x}} = \left[\mathrm{x}_1^1, \mathrm{x}_2^1, \ldots, \mathrm{x}_{\mathrm{n}}^1, \mathrm{x}_1^2, \mathrm{x}_2^2, \ldots, \mathrm{x}_{\mathrm{n}}^2, \ldots, \mathrm{x}_1^{\mathrm{t}}, \right. \\ &\quad \left. \mathrm{x}_2^{\mathrm{t}}, \ldots, \mathrm{x}_{\mathrm{n}}^{\mathrm{t}}\right]^{\mathrm{T}} \in \mathbb{R}^{\mathrm{n}} \end{aligned} \tag{1}$$

where, $\mathrm{f}_1^{\mathrm{t}}(\vec{\mathrm{x}}), \mathrm{f}_2^{\mathrm{t}}(\vec{\mathrm{x}}), \ldots, \mathrm{f}_{\mathrm{m}}^{\mathrm{t}}(\vec{\mathrm{x}})$ are the proposed m real-valued conflicting objective functions, $\mathbb{R}^{\mathrm{m}}$ shows the objective function space, $\mathrm{h}_{\mathrm{i}}^{\mathrm{t}}(\vec{\mathrm{x}})$ and $\mathrm{g}_{\mathrm{i}}^{\mathrm{t}}(\vec{\mathrm{x}})$ are p and $\mathrm{p}-\mathrm{q}$ non-linear equality and inequality constraints for the t^{th} time slot and $\vec{x}$ is the n-dimensional decision vector of the optimization problem for the entire time horizon. In the proposed constrained multi-objective optimization problem (CMOP), the i^{th} degree of constraint violation at a given decision vector $\vec{\mathbf{x}}$ can be computed as;

$$\mathrm{c}_{\mathrm{i}}\left(\vec{\mathbf{x}}\right) = \begin{cases} \max\left(0, \mathrm{h}_{\mathrm{i}}\left(\vec{\mathbf{x}}\right)\right), & \forall \mathrm{i} \leq \mathrm{p} \\ \max\left(0, \left|\mathrm{g}_{\mathrm{i}}\left(\vec{\mathbf{x}}\right) - \epsilon\right|\right), & \text{else} \end{cases} \tag{2}$$

whereas ϵ is the tolerance value used to relax the equality constraints. Usually, in most MOEAs, the degree of overall constraint violation (CV) for all the constraints is computed as;

$$\mathrm{CV}\left(\mathrm{x}\right) = \sum_{\mathrm{i}=1}^{\mathrm{q}} \mathrm{c}_{\mathrm{i}}\left(\vec{\mathbf{x}}\right) \tag{3}$$

Decision vector $\vec{\mathbf{x}}$ is feasible is a feasible search space if a $\mathrm{CV}(\vec{\mathbf{x}})$ is zero, or else it is an infeasible solution. The following sub-sections describe mathematical models of objective functions, constraints, and decision variables for the optimal site and size of DG allocation, along with network reconfigurations.

A. OBJECTIVE FUNCTIONS

In this paper, three objective functions are formulated to find the decision variables of ONR and DG allocation considering

multiperiod time slots. The selection of objective functions is based on economical, technical, and reliability points of view. The first objective function is based on an economical perspective, and it minimizes the cost of energy supplied in the entire time horizon, which can be calculated as:

$$f_1\text{: Cost} = \sum_{t\in T_n}\left(C^t_{SS}\left(P^t_{SS}\right) + \sum_{i\in N_{DG}} C^t_{DG_i}\left(P^t_{DG_i}\right) - \sum_{j\in N_{BESS}} C^t_{BESS_j}\left(P^t_{dch_j}\right)\right) \quad (4)$$

where indices t and i show the particular time interval and DR (distributed Resource) number, respectively. T and N_{DG} are the total time and total number of distributed generators. C_{sub} and C_{DG} The cost parameters of active power supplied by substation and DGs are measured in \$/MWh.

The price of the DG output power is calculated from the second-order quadratic expression as:

$$C_{SS}\left(P_{SS}\right) = k_1 \times P_{SS} \quad (5)$$

$$C_{DG}\left(P_{DG}\right) = k_1 \times P^2_{DG} + k_2 \times P^1_{DG} + k_3 \quad (6)$$

$$C_{BESS}\left(P_{Ch}\right) = k_1 \times P^2_{Ch} + k_2 \times P^1_{Ch} + k_3 \quad (7)$$

where C_{DG}, C_{ESS}, and C_{loss} are the expressed DGs costs, charging the cost of ESSs, and cost of energy loss. k_1, k_2 and k_3 DG, BESS, and energy loss are the variable quadratic cost coefficients. The second objective function considers the economic and technical aspects and calculates the energy loss (CEL) cost in the entire time horizon using Equation (8).

$$f_2\text{: CEL} = \sum_{t\in T}\left(\alpha^t\left(P_{loss}\right)\right) \quad (8)$$

whereas α^t is the parameter for the cost measured in \$/MWh, P_{loss} is the total active power loss in the entire time horizon. Active power loss can be calculated as:

$$P_{loss} = \sum_{t\in T}\left(P^t_{loss}\right) \quad (9)$$

$$P^t_{loss} = \sum_{(s,r)\in nl} G_{sr}\left(V^2_s + V^2_r - 2V_sV_r\cos\left(\theta_{sr}\right)\right) \quad (10)$$

Meanwhile, nl shows the total number of branches, and (s, r) is the particular branch between bus s and r. V_m and V_k are the bus voltages and G_{sr} is the branch conductance connected between bus s and r and θ_{sr} is the branch voltage angle difference between bus angles θ_s and θ_s. And α is the Power loss co-efficient equal to 80.49 \$/MWh [21].

Nodal voltage magnitude is an important indicator to evaluate system security and power quality (PQ). Minimizing voltage deviation can help guarantee better voltage levels in the power distribution systems. The third objective function is related to the security of the distribution network, which is achieved by minimizing voltage deviation (VD) between bus and reference bus voltage that can be calculated as given in Equation (11).

$$f_3\text{: VD} = \sum_{t\in T}\left(\sum_{m\in N_L}|V_{SS} - V_m|^2\right) \quad (11)$$

where m is the particular bus number, and N_b are the total number of buses in the network. V_{ref} is the voltage at slack bus, and it is set to 1 p.u in this paper. V_m is the voltage at a specific bus. Whereas, $C^t_{sub}, C^t_{DG_i}$ and C^t_{loss} are the cost parameters of power supplied by the substation, DGs, and losses in the branch. N_{DG}, N_l, and N_b show the total number of dispatchable and non-dispatchable DGs, branches, and buses, respectively, and i, l,and b are the indices of each DG, branch, and bus.

B. CONSTRAINTS

1) CONSTRAINTS OF EQUALITY AND INEQUALITY

The equality constraints are the equations that ensure a balance of power in the network, where both the active and reactive power generated must be equal to the load demand and losses in the network.

$$\sum_{t\in T}\left(P^t_{SS} + \sum_{i\in N_{ESS}} P^t_{dch_i} + \sum_{i\in N_{DG}} P^t_{DG_i} - \sum_{b\in N_b}\left(P^t_{D_b} + P_{loss}\right) - \sum_{i\in N_{ESS}} P^t_{ch_i}\right) = 0 \quad (12)$$

$$\sum_{t\in T}\left(Q^t_{SS} + \sum_{i\in N_{DG}} Q^t_{DG_i} - \sum_{b\in N_b}\left(Q^t_{D_b} + Q_{loss}\right)\right) = 0 \quad (13)$$

where, P_{sub} and Q_{sub} does the mainstream sub-station supply the active and reactive power, P_D and Q_D are the active and reactive demand, P_{loss} and Q_{loss} presents the active and reactive power loss in the network. $P^t_{ch_i}$ and $P^t_{Dch_i}$ shows the charging and discharging power of energy storage devices.

2) INEQUALITY CONSTRAINTS

The inequality constraints are the operating limits of the equipment, components in the power system, and security constraints on the line and load buses.

$$P^{min}_{SS} \le P_{SS} \le P^{max}_{SS}; Q^{min}_{SS} \le Q_{SS} \le Q^{max}_{SS} \quad (14)$$

$$P^{min}_{DG_i} \le P_{DG_i} \le P^{max}_{DG_i}; Q^{min}_{DG_i} \le Q_{DG_i} \le Q^{max}_{DG_i} \quad (15)$$

$$\sum_{i\in N_{DG}} P_{DG_i} \le \sum_{j\in N_b} P_{D,j} \quad (16)$$

$$\sum_{i\in N_{DG}} Q_{DG_i} \le \sum_{j\in N_b} Q_{D,j} \quad (17)$$

$$V^{min}_{DG_i} \le V_{DG_i} \le V^{max}_{DG_i} \quad (18)$$

$$V^{min}_m \le V_m \le V^{max}_m \quad (19)$$

$$S^t_l \le S^{max}_l \quad (20)$$

$$n_l = N_b - 1 \quad (21)$$

$$\det(\mathbf{A}) = \begin{cases} 1\ or\ -1, & \text{(radial network)} \\ 0 & \text{(not radial)} \end{cases} \tag{22}$$

$$SoC_j^t = SoC_j^{t-1} + \frac{\eta_j P_{dch_j}^t}{E_j^{max}} - \frac{P_{ch_j}^t}{\eta_j E_j^{max}} \tag{23}$$

$$SoC_{j(ini)} = SoC_j^{t-1} = 1.8\ \text{MWh} \tag{24}$$

$$0.1 * E_j^{max} \le SoC_j \le 0.9 * E_j^{max} \tag{25}$$

$$0 \le P_{ch_j}^t \le 0.5\text{MW and } 0 \le P_{dch_j}^t \le 0.5\text{MW} \tag{26}$$

where the state of charge (SoC) of the BESS for each time step shown with SOC_i^t. Note that BESS units' charging and discharging phases are identical to avoid the internal energy exchange between BESS units at each time interval. References [64], [65], E_i^{max} maximum capacity of the storage device that is set to 1.8 MWh.

Equations (14) and (15) define the main substation's active and reactive power limits, identified as the reference bus in this analysis. Equations (16) to (17) set forth the cumulative power constraints of Distributed Generators (DGs), ensuring the total active and reactive power generated remains within or equal to the total demand. Voltage constraints for the PV and PQ buses are addressed in Equations (18) and (19), respectively, while Equation (20) pertains to the MVA branch flow limit. Equations (21) to (22) establish the radiality constraints of the distribution system, ensuring its tree-like structure. Matrix A, the connection matrix or branch and bus incident matrix, plays a pivotal role in network configuration, where $A_{ij} = 1$ indicates that the ith branch is linked from bus j, $A_{ij} = -1$signifies that the ith branch is connected to bus i and $A_{ij} = 0$ confirms no connection between the ith branch and jth bus. Equations (24) to (26) outline the inequality constraints for the Battery Energy Storage Systems (BESS), representing intertemporal constraints linked to various periods. The forward-backward sweep method is utilized for load flow calculation, ensuring all equality constraints specified in Equations (12) and (13) are adhered to. In contrast, the inequality constraints detailed in Equations (14) to (26) are managed using the Representative Constrained Domination Principle (CDP), a constraint handling technique elaborated in section IV of this paper. This comprehensive approach ensures a robust and efficient optimization of the power distribution network.

3) DECISION VECTOR

In this paper, the Decision vector x comprises continuous and integer variables. Mathematically, the vector x is given as.

$$x = [site_{DG,S}, size_{DG,S}, site_{DG,W}, size_{DG,W}, site_{BESS}, size_{BESS}, V_{DG}, CB_L] \tag{27}$$

In this paper, the decision vector shown in Equation (27) comprised of the site of wind type DG $site_{DG,W}$, size of wind type DG $size_{DG,W}$, site and size of solar PV type DG $site_{DG,S}$, $size_{DG,S}$ respectively, the voltage set point of all the generator buses V_{DG}, and selection of tie switches CB_L this variable is set to the number of loops in the network. The decision vector is comprised of integer and continuous variables.

III. IMPLEMENTATION OF I-BICO ALGORITHM FOR ONR AND DG ALLOCATION

ONR and DG allocation are multi-objective mixed integer non-linear problems that challenge the existing MOEAs due to their small feasible search space and constraints in both the objective and control variable space. To address this lacuna, this paper proposes an I-BiCo-constrained MOEA that employs the constraint domination principle (CDP) to handle constraints. In this paper, the CDP is employed, which is a simple and efficient constraint handling technique (CHT) [63], and it compares the pairs of individuals using the following rules:

- If both solutions $\vec{x}_u$ and $\vec{x}_v$ are infeasible, select $\vec{x}_u$ if $CV(\vec{x}_u) < CV(\vec{x}_v)$.
- $\vec{x}_u$ is feasible and $\vec{x}_v$ is infeasible, select the feasible one, i.e., $\vec{x}_u$.
- If both $\vec{x}_u$ and $\vec{x}_v$ are feasible, then select $\vec{x}_u$ if for all the objective functions $f_i(\vec{x}_u) \le f_i(\vec{x}_v)$.

A. IMPLEMENTATION OF MULTI-OBJECTIVE IMPROVED BIDIRECTIONAL COEVOLUTIONARY (I-BICO) ALGORITHM

Multiperiod ONR, along with DG allocation, is a mixed integer-constrained non-linear large-scale distribution problem. It is challenging for the MOEAs to achieve a well-converged and evenly distributed Pareto Front (PF).

In the literature, most of the existing MOEAs prioritize feasible solutions, leading to two issues: firstly, the population may become stuck in local optimal feasible regions. Second, since the population only grows on the feasible side, the search space may not be entirely explored. The conventional approach of optimizing feasible solutions may only result in the population being trapped in local feasible or optimal feasible regions, limiting its ability to efficiently drive the solutions towards the true or global PF. To overcome these issues, an I-BiCo algorithm [66] along with the integration of CDP [63] is proposed in this paper, which coevolves both feasible (main) and infeasible (archive) populations to drive the solutions towards the PF. This is achieved by searching the space from both the feasible and infeasible sides of the search space. In addition, a novel angle-based density (AD) selection technique is developed to update the archive population. This scheme preserves the diversity of the search space, makes it easier to find more feasible regions, and keeps the infeasible solutions close to the PF. Four steps can be used to explain the I-BiCo algorithm. First, a random beginning population is generated, and each population's goal functions and overall constraint violation (CV) are assessed. The second stage entails creating an offspring population (Q_t) by cooperating and interacting between the archive (promising infeasible solutions) and main (feasible search space) populations to create high-quality offspring. In a binary tournament, parents

are chosen for the mating pool. Parents are picked from the combined population of the main (P_t) and archive (A_t) populations if the length of the archive population ($\|A_t\|$) is less than population size N. Otherwise, the main and archive populations are contrasted using angle-based density (AD) and constraint violation, respectively, to pick the parents. Two solutions, x_1 and a_1, are picked at random from P_t and A_t, respectively, to determine the parent p_1, the solution with the smallest CV value is chosen. The random selection of x_2 and a_2 from P_t and A_t respectively, yields the choice of p_2, which is the one with the larger AD value. The following is how the proposed algorithm determines AD. The proposed algorithm obtains AD as given below:

In the opening, normalize the objective function space, say jth solutions of objective functions $F'_i(v_j) = (f'_1(v_j), f'_2(v_j), \ldots, f'_m(v_j))$ using ideal Z^i_{min} and nadir Z^i_{max} points in the combined population U_t according to;

$$f'_i(x_j) = \frac{f_i - Z^i_{min}}{Z^i_{max} - Z^i_{min}}, \quad i = 1, 2, \ldots, m \tag{28}$$

After that, the vector angle between $F'(x_j)$ and $F'(x_k)$ solutions selected from U_t is computed as

$$\theta'_{x_j,x_k} = \arccos\left|\frac{\mathbf{F}'(x_j)\cdot\mathbf{F}'(x_k)}{\|\mathbf{F}'(x_j)\|\,\|\mathbf{F}'(x_k)\|}\right| \text{where} x_k \in \mathcal{P}_t \cap x_k \neq x_j \tag{29}$$

Next, each solution is ranked based on the angle between them. The larger the angle, the higher the rank of the solution, making it a promising candidate for mating selection. The third step involves updating the main population P_{t+1}, which drives the search toward the PF from the feasible side of the search space. To do this, the main population is combined with the offspring population Q_t, and solutions are divided into feasible S_1 and infeasible S_2 sets. If the number of feasible solutions in S_1 is less than the population size N, then the first $(N-S_1)$ infeasible solutions from the sorted set S_2 are selected. If the number of feasible solutions in S_1 is greater than N, non-dominated sorting is applied to S_1 to obtain the PF of different ranks, such as $\mathcal{F}_1, \ldots, \mathcal{F}_k$, and so on, where $\mathcal{F}_1$ is the highest rank. The solutions with the highest rank are assigned to P_{t+1}, followed by the second-highest rank, and so on until the size of P_{t+1} is equal to N or greater than N. If the size of P_{t+1} exceeds N, then the crowding distance (CD) operator is used to eliminate some of the solutions in the last front [63]. The fourth and final step involves updating the archive population for the next iteration A_{t+1}, The accountable entity for developing non-dominated, infeasible solutions is aimed at enhancing the variety of the Pareto front [66]. The algorithm considers CV as an additional objective function $M+1^{th}$, making the original constrained problem an unconstrained multi-objective problem, given as:

$$\min F(x) = (f_1(x), f_2(x), \ldots, f_m(x), CV(x))^T \tag{30}$$

This helps in generating promising, non-dominated, infeasible solutions. Next, the solutions are ranked using ND sort [63] to determine the PF, and capable infeasible solutions are selected based on CV (M+1 objective function) and AD as described in Equation (28). Figure 1 displays the flow diagram of the proposed algorithm.

IV. MODELING OF TIME-VARYING DEVICES AND STUDY CASES

This paper has optimized multiperiod ONR and the optimal DR allocation problem using an I-BiCo Algorithm. The optimal site and size of RES-type DGs and BESS are considered. Non-dispatchable solar PV type DGs are implemented to integrate active power only (operate at unity pf). However, wind-type DGs locally inject variable reactive power that highly supports the voltage profile of the distribution system and reduces active power loss to some extent. The simulations are conducted on the 33 IEEE bus power system, as illustrated in Figure 2. The optimization period is 72 h for each representative summer, winter, and spring/fall day) to account for the seasonal effects. Forecasted RES active power integration and load demand for the entire time period are shown in Figure 3. At first, base-case load flow calculations are performed for the test systems without DR sources. Active power losses in selected days of 24 hours are found to be 4.215 MW per day. The base kV and MVA of the proposed test network are 12.66kV and 10 MVA; usually, it has five tie switches allocated at 33, 34, 35, 36, and 37 branches. The corresponding line impedances and the active and reactive power can be found in Ref. [67], with the increased active power load demand shown in Figure 3 (b).

The energy loss for each time frame is determined by performing a load flow analysis for each period, considering the average load and distributed generation (DG) output for the corresponding period. This analysis is based on the network configuration established through the optimization process for the specific time frame. The data associated with the installed DGs, and BESS are taken from [67] and [68].

Three solar PV and three wind generators of 1MW rated capacity each are selected to be installed at the optimal site of the 33-bus test system. Six BESS are installed with having maximum capacity of 1.8 MWh each with the minimum and maximum charging and discharging capacity of 0.5 MW each are selected to be installed in the proposed test system. In this research paper, we offer a simultaneous solution to the optimization problem of network reconfiguration and optimal allocation of both DGs and BESS. Furthermore, the time-varying nature of the load recognizes that the optimization problem in existing literature typically assumes a constant power generation model for renewable DGs. By accounting for the time variation in both load and DG generation, we aim to provide network managers with a more accurate and realistic solution for optimal network configuration and DG sizes and locations. To achieve this, we calculate the hourly power outputs of solar PV and wind-type DGs using their respective power generation func-

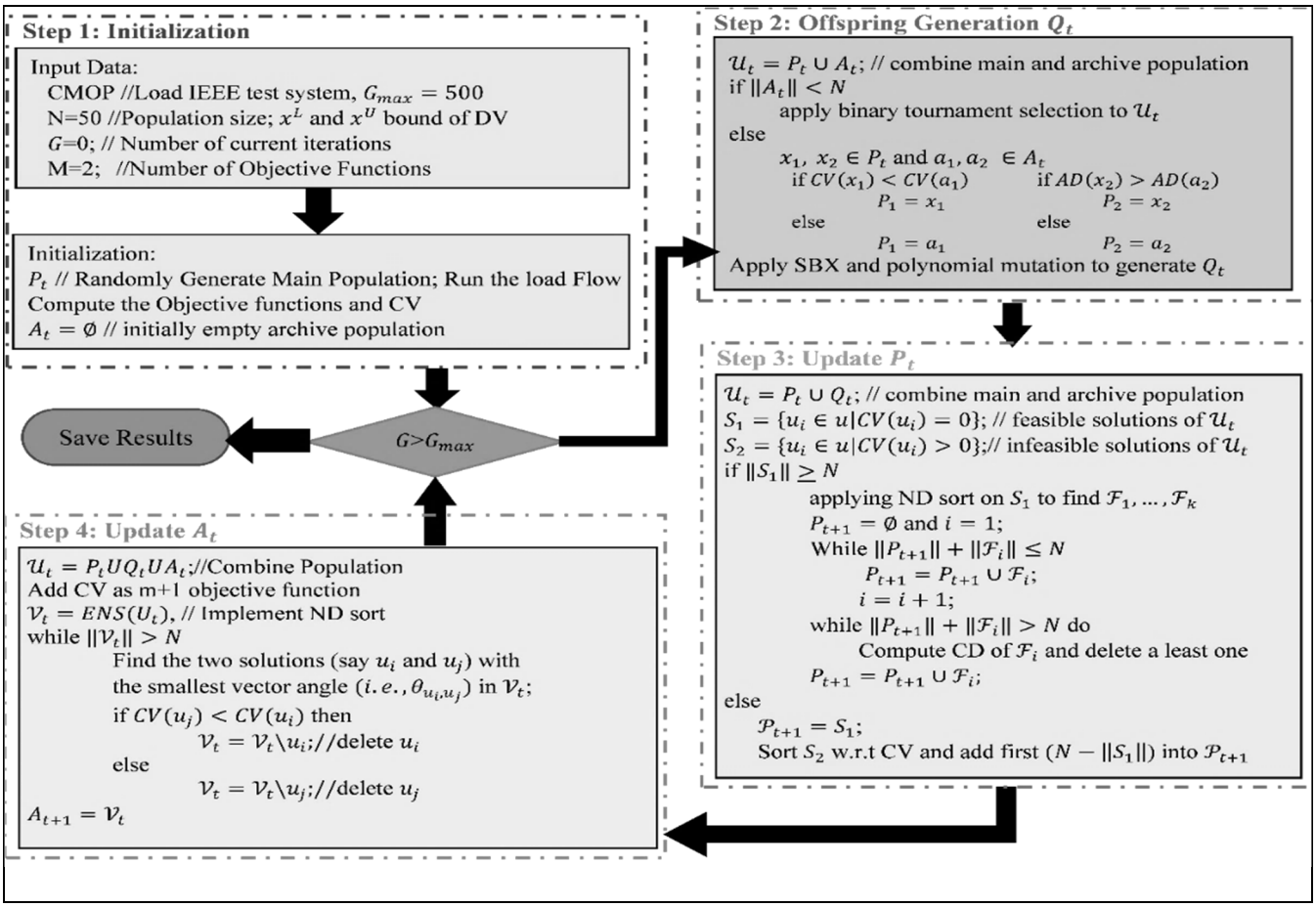

FIGURE 1. Flow diagram of the proposed algorithm.

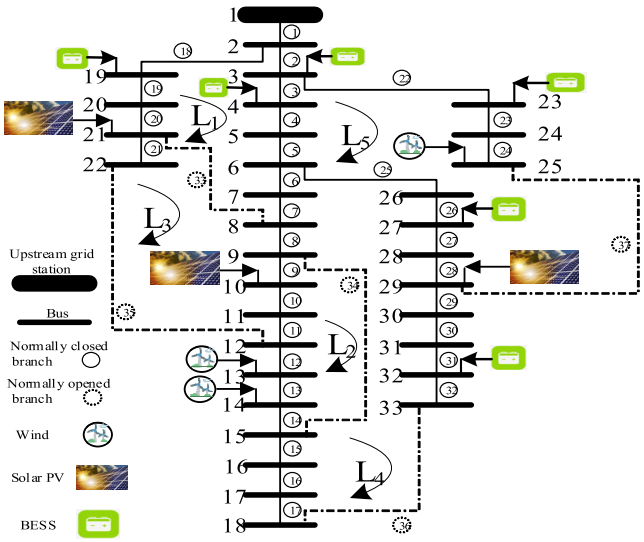

FIGURE 2. Layout of proposed IEEE 33-bus network.

tions alongside load forecasts for an average day during the summer season, which serves as the reference period for our optimization study. The curves of the hourly variance in a load of an average summer day as an example of study along with the variable market price of power produced by the grid, output power of solar PV type DG, and actual active and reactive demand converted from p.u load curve are illustrated in Figure 3 (a), (b).

The proposed formulation finds the scheduling of grid energy supplied according to load variation and the DGs' rated power. The proposed problem is resolved with the I-BiCo algorithm, aiming to simultaneously reduce two and three competing objective functions as specified in Equations (4), (8), and (11) that are the total cost of energy supplied (f_1), cost of energy loss (f_2) and voltage deviation (f_3) in the entire time horizon. We consider the two scenarios for testing our proposed method for finding the realistic multiperiod optimal network reconfiguration and DG and BESS allocation in a multi-period time horizon.

Scenario 1: Optimal site and size of DG along with BESS without reconfiguration

Scenario 2: Optimal site and size of DG and BESS with optimal network reconfiguration ONR

Each scenario is run on two study cases comprised of bi-objective and tri-objective functions to find the various

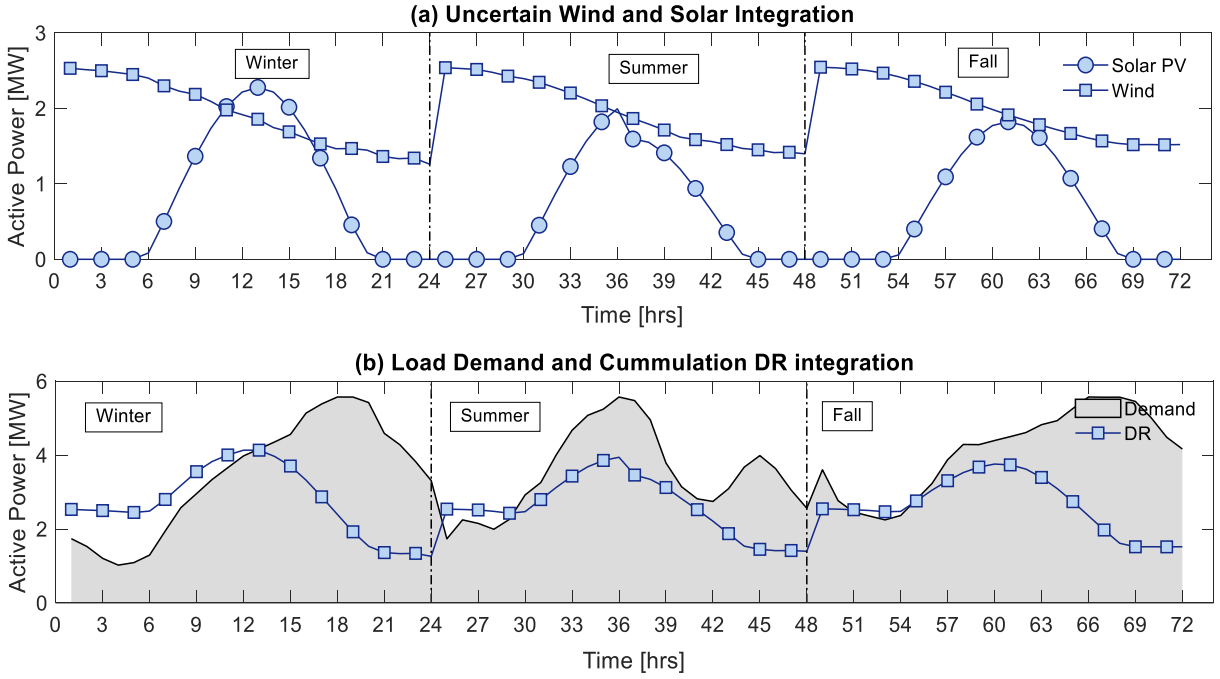

FIGURE 3. Time-dependent input quantities: a) Cumulative uncertain integration of three wind and three solar PV generation, b) Load demand and cumulative DG injection.

decision variables. These study cases are included of Simultaneous minimization of:

Case 1: Total cost of energy supplied by grid station Vs. cost of energy loss.

Case 2: Total cost of energy supplied by grid station Vs. cost of energy loss Vs. VD. The simulation results are discussed in the next section from the point of intended objectives and Pareto front characteristics. The Pareto optimal solution of the proposed bi and tri objective function is determined using the I-BiCo Algorithm. The proposed approach for simultaneously optimizing network reconfiguration and integration of DR is implemented using MATLAB's environmental programming. All experiments in this article were conducted on the platform developed by Tian et al. (PlatEMO) [69]. All the codes are run on corei7 PC MATLAB 2021b version 9.10.

V. ANALYSIS OF SIMULATION RESULTS AND COMPARISON OF SCENARIOS

The optimal site and size of DG and BESS is a constrained multi-objective optimization problem (CMOP) involving conflicting objective functions and various dynamical constraints. Due to constraints, CMOPs' Pareto-optimal solutions will likely lie on constraint boundaries. The ultimate goal of MOEAs is to obtain well-converged and evenly distributed PF. However, it is difficult to achieve that goal, primarily because of constraints. Multi-objective evolutionary algorithms (MOEAs) aim to find high-quality, non-dominated solutions in a single simulation run.

A. COMPARISON OF PROPOSED ALGORITHM WITH THE OTHER MOEAs

Quality measurement of non-dominated (ND) solutions consists of three objectives: i) convergence means minimum distance between the ideal point and PF, ii) diversity final non-dominated solutions are evenly distributed and maximum spread. Performance assessment of MOEAs should take all of these objectives into account. Researchers have spent considerable effort evaluating the goodness of a solution set obtained by MOEAs. It means that the final non-dominated solutions of MOEAs must have better convergence, diversity, and spread. For a fair comparison between the MOEAs, various performance metrics have been proposed in the past. In this work, convergence, and diversity measures of different MOEAs have been done using a well-known hypervolume indicator (HVI) performance metric. HVI metric requires a reference point (preferably a point close to the nadir point) that is [1 1 1] for the normalized objective functions. On a given problem, when comparing different PFs, the PF with the largest HVI is considered the best. To access the performance of the proposed I-BiCo algorithm, it is compared with the recently implemented MOEAs at each iteration. The parameters of all the compared algorithms were kept identical to their original papers. Whereas population size N in all the cases is 40, and 5000 maximum number of iterations (G) are adopted. Statistical performance based on HVI of the proposed algorithm compared with the other recently designed state-of-the-art MOEAs of all the cases and the simulation results are summarized in Table 2.

TABLE 2. Statistical comparison of state-of-the-art MOEAs with the proposed algorithm at 100% FR.

			BCS			Minimum of (f_1, f_2, f_3)			Maximum of (f_1,f_2,f_3)		
		HV	f_1	f_2	f_3	f_1	f_2	f_3	f_1	f_2	f_3
SC1: Case 1	NSGAII [63]	0.789	**1.241E+06**	3.235E+05	--	**1.236E+06**	3.232E+05	--	**1.252E+06**	3.239E+05	--
	CMOQMLT [71]	0.795	1.290E+06	1.067E+05	--	1.290E+06	1.067E+05	--	1.292E+06	1.069E+05	--
	CCMO [72]	0.784	1.367E+06	9.642E+04	--	1.365E+06	9.627E+04	--	1.369E+06	9.666E+04	--
	Proposed	**0.805**	1.249E+06	**4.888E+04**	--	1.249E+06	**4.880E+04**	--	1.253E+06	**4.927E+04**	--
SC1: Case 2	NSGAII [63]	0.733	1.584E+06	2.747E+05	1.081E+00	1.584E+06	2.625E+05	3.951E-01	1.670E+06	4.273E+05	1.380E+00
	CMOQMLT [71]	0.733	1.595E+06	2.721E+05	5.926E-01	1.585E+06	2.378E+05	4.503E-01	1.679E+06	3.154E+05	8.034E-01
	CCMO [72]	0.732	1.602E+06	3.425E+05	4.831E-01	1.559E+06	3.272E+05	4.431E-01	1.653E+06	4.567E+05	8.014E-01
	Proposed	**0.760**	**1.437E+06**	**1.991E+05**	**3.961E-01**	**1.433E+06**	**1.901E+05**	**3.795E-01**	**1.482E+06**	**2.123E+05**	**4.289E-01**
SC1: Case 1	NSGAII [63]	0.718	1.283E+06	1.113E+05	--	1.282E+06	1.104E+05	--	1.299E+06	1.116E+05	--
	CMOQMLT [71]	0.712	1.283E+06	1.802E+05	--	1.280E+06	1.797E+05	--	1.295E+06	1.806E+05	--
	CCMO [72]	0.712	1.313E+06	**1.047E+05**	--	1.311E+06	**1.045E+05**	--	1.316E+06	**1.051E+05**	--
	Proposed	**0.722**	**1.265E+06**	1.079E+05	--	**1.262E+06**	1.071E+05	--	**1.282E+06**	1.082E+05	--
SC1: Case 2	NSGAII [63]	0.712	1.560E+06	2.905E+05	4.615E-01	1.547E+06	2.905E+05	1.673E-01	1.632E+06	3.728E+05	8.537E-01
	CMOQMLT [71]	0.694	1.561E+06	4.645E+05	7.350E-01	1.540E+06	4.316E+05	5.638E-01	1.656E+06	5.710E+05	9.294E-01
	CCMO [72]	0.701	1.563E+06	3.771E+05	5.934E-01	1.555E+06	3.573E+05	3.707E-01	1.633E+06	4.414E+05	9.343E-01
	Proposed	**0.743**	**1.449E+06**	**1.238E+05**	**1.992E-01**	**1.447E+06**	**1.201E+05**	**1.648E-01**	**1.476E+06**	**1.380E+05**	**2.354E-01**

It is worth mentioning that no constraint violation is observed in any trial run of all case studies. The simulation results presented in Table 2 above indicate that, in the majority of circumstances, the proposed approach performs better or is nearly similar to existing techniques, as determined by the best and worst HV values. In Table 2, bold, dark highlighted results are the best, and half-dark is the second-best value. In both of the scenario's bi-objective and tri-objective functions, the proposed algorithm finds the maximum HV values compared to all the other MOEAs. Regarding the best compromise solution (BCS), in SC1 of Case1, NSGAII [63] finds the best value of objective functions 1; however, the proposed algorithm is at second. In the same SC1 and Case 1, the proposed algorithms outperform in terms of the second objective function. The proposed algorithm finds the least minimum and maximum second objective, and the second best is obtained in CCMO [71]. However, the best value of f_1 The minimum and maximum values are obtained in NSGAII. In both scenarios, SC1 and SC2, considering minimizing complex tri-objective functions, the proposed algorithm outperforms all the other MOEAs. The second best, in most cases, is found in NSGAII. From the statistical Table 2, it is shown that the proposed algorithm outperforms compared to most of the MOEAs in both the Cases of SC1 and SC2. From the statistical simulation results, the comparative performance of MOEAs from the first to the last iteration. At each iteration, hypervolume indicators (HVIs) are employed to assess the efficacy of multi-objective optimization algorithms (MOEAs). Multi-objective optimization involves optimizing multiple conflicting objectives simultaneously, and the goal is to find a set of solutions that represents a trade-off among these objectives. HVIs provide a quantitative measure of the quality of the solutions obtained by a MOEA regarding the volume they cover in the objective space. Moreover, HVI measures the volume of the dominated space between the Pareto front (set of non-dominated solutions) and a reference point in the objective space at each iteration. The higher the hypervolume, the better the performance of the algorithm, as it indicates the obtained solutions cover a larger portion of the objective space. Therefore, Figure 4 shows the convergence based on HVI in all the iterations. Analyzing the convergence curve, it becomes evident that, in most cases, NSGA initially converges faster; however, after half of the iterations, the proposed algorithm outperforms by achieving superior Hypervolume (HVI) values. This is attributed to the proposed algorithm's convergence strategy, which selects representative infeasible solutions while HV plots only the feasible solutions. As the iteration progresses, a significant portion of the population becomes feasible, leading to the rapid convergence of HV in the proposed algorithm compared to other MOEAs.

B. FINAL PARETO FRONT AND ANALYSIS OF BEST COMPROMISE SOLUTION

The optimization of the suggested multi-objective problem occurs for the entire time sequence within a single simulation run. This comprehensive approach considers the time sequence variance in renewable DGs and load, exemplified by a typical summer day. A comparison of final non-dominated solutions in the objective space, called Pareto Front (PF), of the proposed algorithm with the other MOEAs for all the study cases is depicted in Figure 5.

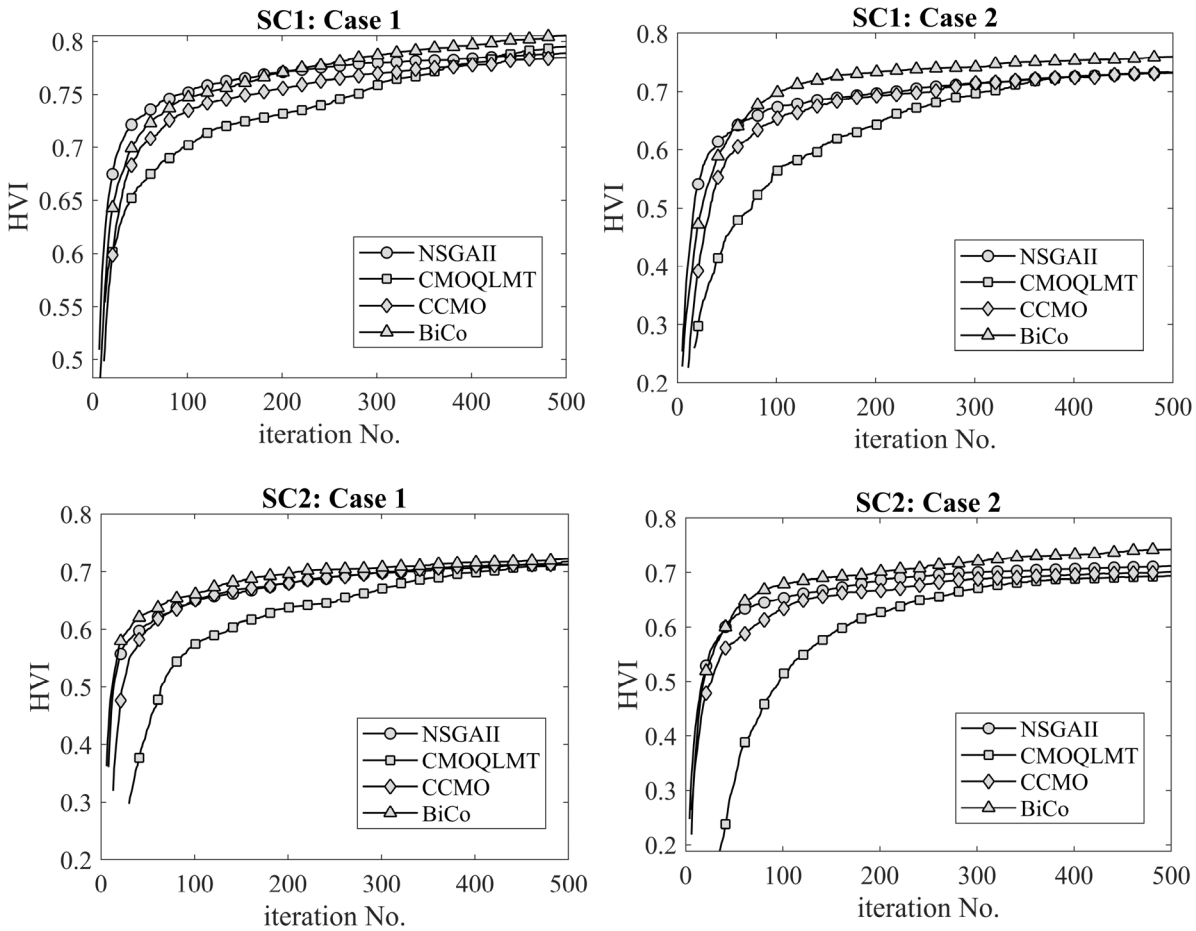

FIGURE 4. Convergence comparison HV of state-of-the-art method from initial to final solution.

Figure 5 demonstrates the ability of the proposed algorithm to effectively balance conflicting objective functions in a complex distribution system problem. In SC1 of Case1, both CCMO [71] and CMOQLMT [70] are stuck in local optimal; however, NSGAII [63] finds the minimum value of f_1. SC1 of Case2, the PF of the proposed algorithm outperforms compared to CCMO [71], NSGAII [63], and CMOQLMT [70], which are stuck in the local optimal solution. PF of most of the MOEAs doesn't converge due to dimensions of decision variables. In the proposed optimization problem, there are 744 decision variables in both cases of SC1 and 864 decision variables in SC2. In Figure 5, the best compromise solution (BCS) [72], with the slightly larger marker size, is considered the best solution in the entire population of the final non-dominated solution that simultaneously provides the optimal values of objective functions without discrimination. In this case, the fuzzy set theory is put forward to help the network manager to extract this best compromise solution, to be applied to the power system, referring to the hour that provides the best values of objective functions. Furthermore, for better visibility Figure 6 shows the trade-off between various objective functions of SC1 and SC2 of proposed algorithm individually.

Figure 6 shows that in Case 1 of SC1 and SC2, population members find the discontinuous PF with the better trade-off between the objective functions. In tri-objective functions, population members are widely distributed, and data tips with larger marker sizes show the BCS. SC1, Case 1 (Top-Left Plot): This plot shows a two-dimensional Pareto front for bi-objective optimization. The axes represent cost and another objective, labeled CEL [$/h]. The population members (depicted as triangles) find a discontinuous Pareto front (PF), indicating gaps in the trade-off curve where no optimal solutions exist. SC2, Case 1 (Bottom-Left Plot): Similar to SC1 Case 1, this plot shows the bi-objective optimization results for a different scenario. The Pareto front is more continuous than SC1, with the population members aligning along a precise trade-off curve. SC2, Case 1 (Bottom-Left Plot): Similar to SC1 Case 1, this plot shows the bi-objective optimization results for a different scenario. The Pareto front is more continuous than SC1, with the population members aligning along a clear trade-off curve. SC2, Case 2

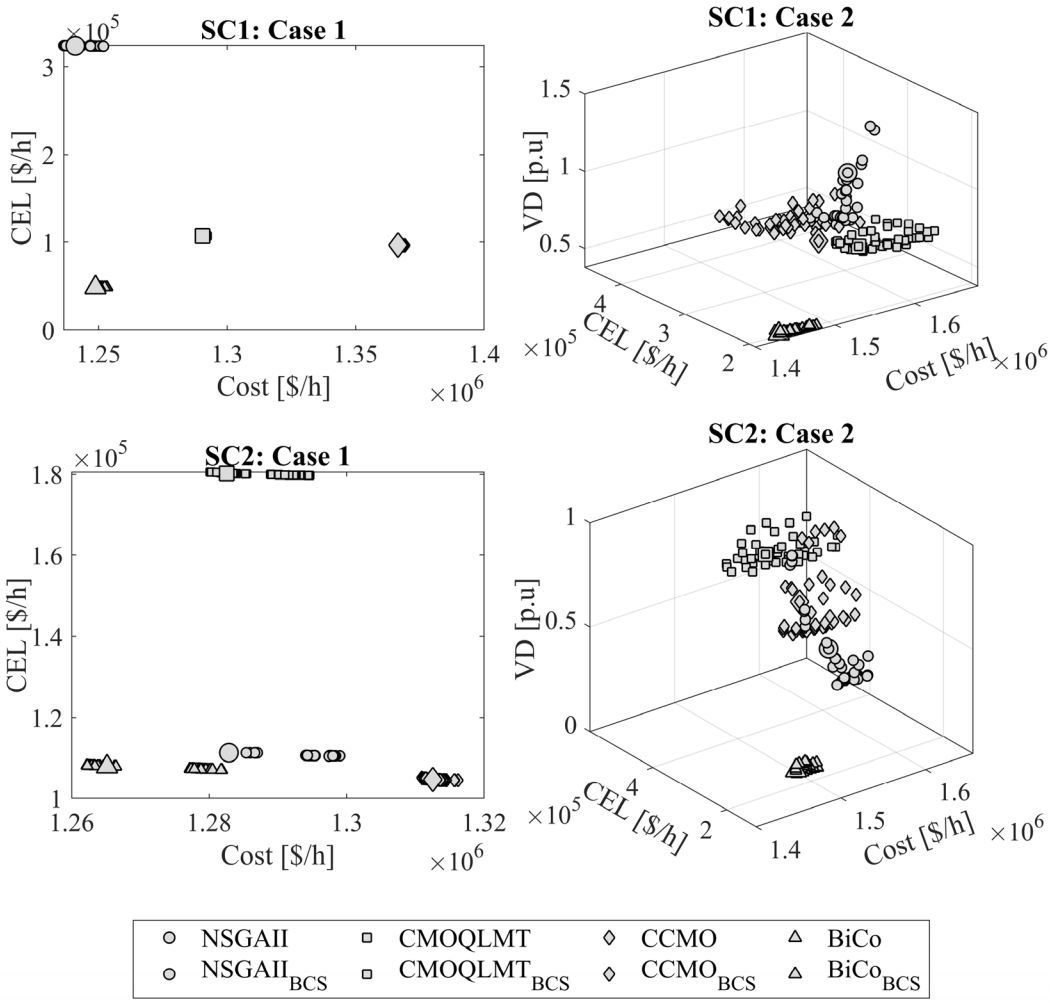

FIGURE 5. Comparison of final non-dominated solution of all the scenarios of bi and tri-objective functions of the proposed algorithm with the state-of-the-art MOEAs.

(Bottom-Right Plot): As in SC1 Case 2, this plot visualizes the tri-objective optimization results for SC2. The distribution of population members again suggests a range of trade-off solutions. The highlighted data point with a more significant marker size represents the Best Compromise Solution (BCS), which indicates the best trade-off solution according to a specific criterion. Table 3 shows the decision variables of BCS of SC1 of both cases, in which tie line switches are fixed: 33, 34, 35, 46, and 37.

Table 3 details the optimal locations and capacities for solar and wind-distributed generators (DGs) and Energy Storage Systems (ESS) without network reconfiguration. It contrasts two cases over 24 hours: Case 1 considers bi-objective functions (total cost of energy from the grid station versus cost of energy loss), while Case 2 adds a third objective function, voltage deviation (VD). For solar DGs in Case 1, the peak generation of 1.77 MW occurs at noon with DGs located at buses 7, 14, and 7, while the minimum generation of 0.07 MW happens at 06:00 and 20:00 hours at buses 30, 24, 8, and 16, 30, 24, respectively. In Case 2, the maximum solar output of 1.757 MW is achieved with DGs at buses 20, 25, and 29; the least generation of 0.062 MW is at 20:00 hours at buses 30, 20, and 19. Solar power is absent outside irradiation periods. Wind turbines (WTs), unlike solar DGs, generate power continuously. In Case 1, WTs at buses 16, 16, and 25 produce a maximum of 2.04 MW at 01:00 hour and a minimum of 1.24 MW at 24:00 hour at buses 24, 30, and 18. For Case 2, the peak of 2.32 MW occurs at 01:00 with WTs at buses 11, 11, and 20, and the lowest output of 1.09 MW at 24:00 hour at buses 33, 28, and 15.

BESS units support the grid by discharging during power deficits and charging when excess power is available, demonstrating varying charge and discharge rates throughout the day. This information is crucial for enhancing energy system efficiency and stability, particularly as the integration of renewable energy sources increases. Table 3 lists the optimal Solar PV and Wind Turbines sites under specific columns, with their sizes indicated in megawatts. Solar PV remains

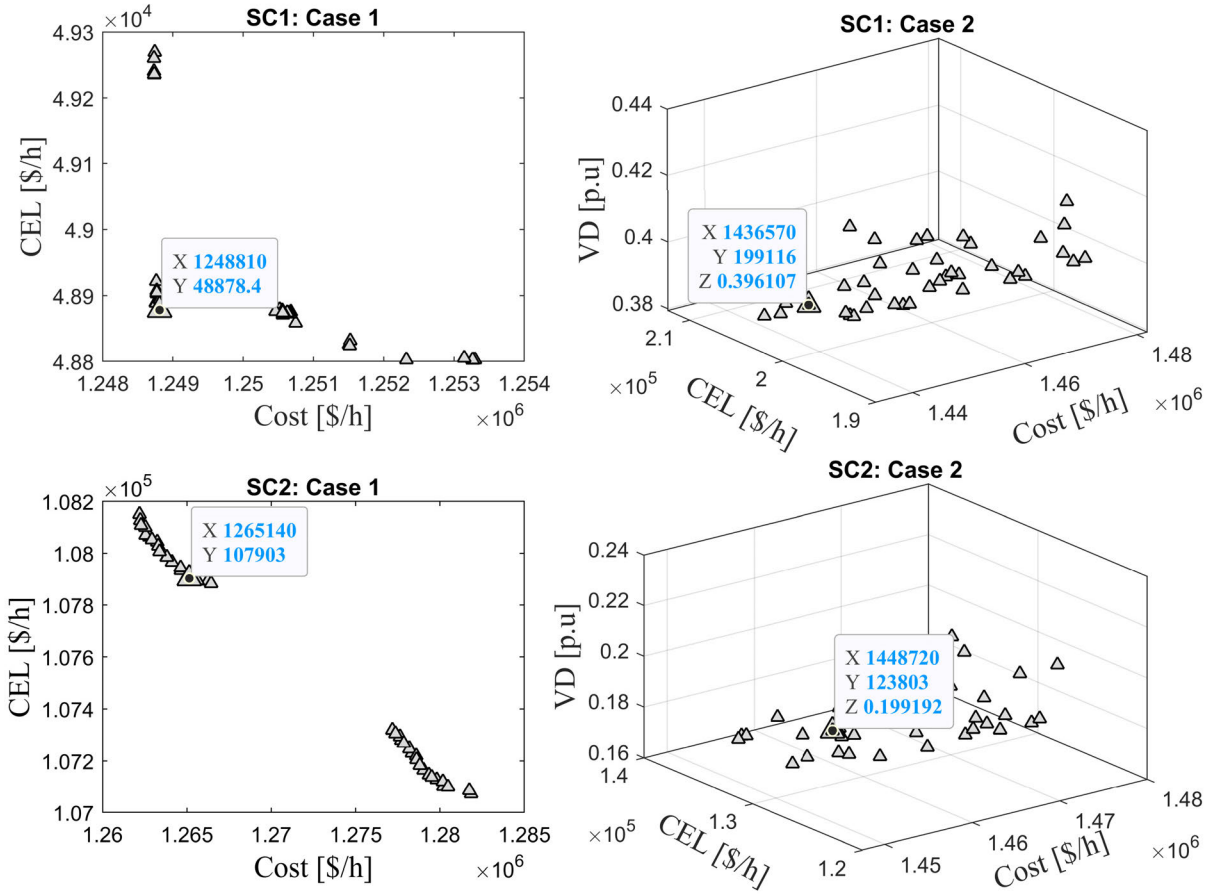

FIGURE 6. Final non-dominated solutions of the proposed algorithm of all the scenarios considering bi-objective and tri-objective functions.

TABLE 3. Optimal site and size of SolarPV and wind DG and ESS (without optimal network reconfiguration).

	Case 1						Case 2					
Time	PV_{site}	$\sum P_{SDG}$ [MW]	WT_{site}	$\sum P_{WDG}$ [MW]	$BESST_{site}$	$BESS_{Size}$ [MW] +ch,−dch	PV_{site}	$\sum P_{SDG}$ [MW]	WT_{site}	$\sum P_{WDG}$ [MW]	$BESST_{site}$	$BESS_{Size}$ [MW] +ch,−dch
1	7,16,30	0	16,16,25	2.04	16,17,32,6,23,25	0.50,-0.45,0.45,-0.30,0.48,-0.05	32,11,6	0	11,11,20	2.32	18,19,14,27,25,32	-0.04,0.40,-0.34,0.16,0.18,-0.45
2	24,33,30	0	28,33,28	1.90	33,29,12,3,28,11	0.32,-0.43,0.13,-0.10,-0.50,-0.14	22,22,33	0	22,18,28	2.06	19,19,25,22,3,17	0.14,-0.04,0.28,-0.32,0.49,-0.35
3	15,8,30	0	27,21,21	1.87	14,29,22,8,21,9	-0.17,0.50,-0.25,0.50,0.39,-0.50	6,18,25	0	18,30,12	2.02	2,16,2,18,28,28	0.35,0.32,-0.42,-0.44,-0.00,0.44
4	33,12,30	0	7,16,24	1.93	12,5,12,19,16,5	-0.21,0.50,0.50,-0.36,-0.28,-0.18	30,10,19	0	17,32,7	2.16	13,32,17,9,32,9	-0.05,0.32,-0.06,0.28,-0.10,-0.46
5	10,18,10	0	26,33,24	1.84	10,10,33,15,7,20	-0.50,0.29,-0.13,-0.10,-0.24,0.00	28,25,31	0	29,13,30	1.99	30,3,29,13,5,27	-0.31,-0.27,0.11,0.41,-0.22,-0.17
6	30,24,8	0.07	8,14,19	1.94	8,32,13,9,14,23	0.36,-0.15,-0.24,0.16,-0.04,-0.18	28,27,26	0.070	9,33,3	1.97	13,11,21,25,13,6	-0.22,-0.11,0.38,-0.26,0.08,0.04
7	30,14,26	0.38	8,24,26	1.84	5,26,30,8,5,30	0.25,0.33,-0.15,0.50,0.42,0.49	17,7,15	0.382	19,6,19	2.08	31,13,8,21,15,32	-0.33,-0.29,-0.25,-0.50,0.50,0.48
8	29,7,29	0.74	10,24,17	1.78	6,21,32,32,6,26	0.44,-0.15,-0.06,-0.50,-0.50,-0.49	31,22,30	0.714	24,18,6	1.93	32,8,30,19,7,8	-0.02,0.38,-0.18,0.32,0.11,-0.16
9	3,22,30	1.05	22,6,14	1.88	22,14,19,11,11,25	-0.45,0.24,-0.25,-0.26,-0.11,0.50	21,30,6	1.082	13,13,24	1.83	31,13,25,17,3,14	-0.13,0.12,0.46,0.50,-0.33,0.49
10	30,3,14	1.30	7,20,25	1.87	3,19,13,13,3,23	-0.34,0.10,-0.22,0.50,-0.37,0.35	18,30,7	1.503	22,25,22	1.73	17,27,22,18,12,15	0.43,-0.34,-0.50,-0.27,-0.50,0.40
11	7,30,24	1.49	11,17,11	1.60	11,11,17,25,14,2	0.35,0.31,0.31,-0.13,0.20,0.11	17,30,13	1.624	20,7,25	1.82	5,13,30,2,30,3	-0.20,-0.18,-0.10,-0.02,-0.12,0.37
12	7,14,7	1.77	30,24,32	1.71	33,26,26,25,21,2	0.10,-0.13,-0.21,0.27,0.24,-0.13	20,25,29	1.757	29,14,14	1.71	8,29,29,6,24,13	0.43,0.23,0.43,0.22,-0.46,-0.48
13	25,15,9	1.57	30,9,25	1.86	5,32,21,21,19,9	-0.33,-0.50,-0.02,-0.50,-0.49,-0.28	13,30,13	1.399	26,24,25	1.56	15,29,15,14,31,31	-0.43,-0.18,-0.47,-0.28,-0.23,-0.35
14	20,30,8	1.55	14,3,25	1.75	26,6,7,5,26,5	0.37,0.15,0.37,0.50,0.49,0.48	30,8,25	1.424	15,20,20	1.48	31,13,13,26,13,21	0.33,-0.27,0.39,-0.29,0.47,0.10
15	25,21,15	1.41	26,30,26	1.69	24,29,10,19,29,29	0.46,-0.49,0.38,-0.48,0.28,0.33	16,7,21	1.326	7,31,25	1.60	9,29,3,15,15,8	-0.31,0.19,0.12,-0.26,0.26,-0.14
16	6,25,30	1.20	10,25,23	1.61	11,32,16,11,16,11	-0.28,0.11,-0.48,-0.37,0.50,-0.23	17,30,25	1.169	12,6,32	1.58	11,20,26,20,11,7	0.49,0.45,-0.32,0.49,-0.42,0.30
17	32,17,32	0.94	12,30,25	1.53	25,26,19,8,25,19	0.50,0.22,-0.37,0.30,-0.18,-0.39	31,25,18	0.885	31,7,18	1.46	22,2,5,2,14,22	-0.43,0.48,0.00,-0.34,-0.02,-0.38
18	5,23,25	0.65	12,25,30	1.47	23,16,33,32,2,23	-0.19,-0.21,-0.49,-0.11,-0.15,-0.12	8,25,33	0.597	33,30,8	1.34	24,2,17,13,16,24	0.38,-0.21,0.23,-0.01,0.39,-0.21
19	25,17,5	0.40	17,30,30	1.47	26,13,13,13,32,13	-0.50,0.23,0.09,0.47,-0.13,0.49	18,30,24	0.358	11,18,24	1.42	32,9,20,33,31,9	0.24,0.04,-0.34,0.47,-0.01,0.50
20	16,30,24	0.07	9,6,16	1.45	25,6,12,12,5,32	-0.50,-0.08,0.37,-0.50,-0.44,-0.50	30,20,19	0.062	3,19,14	1.30	33,10,7,31,14,8	-0.50,-0.49,0.48,0.23,-0.07,-0.39
21	6,6,25	0	30,25,14	1.36	10,9,32,17,6,26	0.44,0.42,0.35,0.47,0.50,0.50	25,8,20	0	16,33,7	1.25	30,11,8,24,8,23	0.48,0.49,0.40,0.09,-0.18,-0.03
22	7,14,19	0	30,7,25	1.33	28,32,28,2,28,2	-0.43,-0.18,-0.32,0.34,-0.50,-0.12	30,19,7	0	3,14,17	1.27	14,32,14,14,30,30	-0.50,0.07,-0.32,-0.50,-0.22,0.01
23	23,24,30	0	14,20,20	1.34	8,11,7,11,7,33	0.47,0.20,-0.12,-0.50,-0.03,-0.45	25,9,9	0	6,16,33	1.27	7,25,6,9,9,25	0.49,-0.39,-0.49,-0.20,-0.24,-0.04
24	6,18,13	0	24,30,18	1.24	11,6,11,32,11,25	0.43,-0.01,-0.50,-0.50,-0.50,-0.50	22,15,22	0	33,28,15	1.09	10,24,17,10,25,4	-0.03,-0.23,0.21,-0.50,-0.50,-0.50
CB_tie	33,34,35,36,37						CB_tiw	33,34,35,36,37				

at 0 MW throughout both cases, signifying no contribution to the generation capacity. In comparison, wind power varies between 1.30 MW and 2.32 MW in Case 1 and 1.09 MW and 2.32 MW in Case 2, reflecting its fluctuating input. BESS sizes also change across the day, illustrating the need for adaptive storage solutions. In rapid, Table 3 provides a snapshot of how renewable energy sources and storage systems are optimally utilized across a day without reconfiguring the network. In contrast, Table 4 presumably extends this analysis to scenarios that include optimal network reconfiguration. Table 4 provides a 24-hour overview of the optimal placement and sizing of solar and wind-distributed generators

TABLE 4. Optimal site and size of SolarPV and wind DG and ESS (with optimal network reconfiguration).

	Case 1						Case 2					
Time	PV_{site}	$\sum P_{SDG}$ [MW]	WT_{site}	$\sum P_{WDG}$ [MW]	$BESST_{site}$	$\underset{+ch,-dch}{BESS_{Size}}$ [MW]	PV_{site}	$\sum P_{SDG}$ [MW]	WT_{site}	$\sum P_{WDG}$ [MW]	$BESST_{site}$	$\underset{+ch,-dch}{BESS_{Size}}$ [MW]
1	15,7,24	0	26,30,5	2.01	2,6,26,33,19,19	-0.32,-0.41,0.30,0.31,-0.50,-0.50	25,22,30	0	7,25,20	2.00	29,14,7,15,32,8	0.15,-0.06,-0.31,0.32,0.47,0.47
2	14,30,12	0	14,14,25	2.01	14,5,3,25,13,21	0.50,0.50,-0.50,0.23,0.39,-0.44	28,24,21	0	18,24,18	2.07	11,18,5,17,23,24	-0.30,-0.09,0.05,0.00,0.49,0.15
3	13,8,24	0	15,20,30	1.96	5,33,26,10,21,9	0.44,-0.15,0.35,0.45,-0.50,-0.19	16,17,12	0	16,30,16	1.92	26,8,26,17,16,20	0.33,0.50,0.31,0.41,-0.49,0.14
4	7,2,7	0	12,30,24	1.95	22,19,30,32,24,32	-0.32,0.50,-0.24,-0.40,-0.32,0.46	32,9,13	0	25,22,9	2.18	30,3,13,4,9,13	0.15,-0.48,-0.11,0.03,-0.22,0.15
5	15,22,6	0	32,4,7	1.94	6,4,7,5,26,30	-0.50,-0.48,0.50,-0.14,0.36,0.04	16,25,22	0	8,21,12	1.97	26,8,2,22,22,28	-0.38,0.31,0.33,-0.16,-0.12,-0.16
6	17,32,9	0.07	30,17,9	1.80	10,32,17,32,18,11	-0.06,0.50,-0.14,0.27,-0.22,0.25	31,21,24	0.08	12,27,14	1.97	12,21,13,22,15,24	0.30,-0.04,-0.15,0.31,0.23,0.09
7	30,16,32	0.39	24,10,21	1.96	19,10,3,31,31,3	0.49,-0.50,0.50,-0.32,0.50,-0.09	3,17,10	0.39	25,23,11	2.01	11,11,6,14,13,31	-0.20,0.38,0.31,-0.49,0.30,-0.09
8	33,30,6	0.69	8,30,6	1.94	3,19,31,6,12,12	-0.23,-0.50,-0.50,-0.07,0.02,0.48	22,24,24	0.75	13,15,31	2.12	11,27,31,15,13,19	0.16,-0.28,-0.26,0.49,-0.46,-0.45
9	30,17,25	0.97	25,12,17	1.84	25,26,13,32,17,13	-0.10,0.48,-0.35,-0.37,0.01,-0.50	15,3,14	1.02	30,9,22	2.00	16,29,9,29,33,18	-0.24,0.39,-0.35,-0.50,-0.48,0.30
10	14,30,26	1.34	10,10,14	1.57	10,25,18,3,14,2	0.46,-0.20,-0.44,0.46,-0.45,-0.17	15,3,2	1.33	20,19,30	1.71	12,14,29,22,32,21	0.50,0.49,0.07,0.50,-0.22,-0.20
11	30,24,13	1.65	15,18,22	1.60	8,4,25,18,4,8	0.35,0.38,0.48,-0.46,0.48,0.34	6,30,16	1.61	16,26,8	1.76	12,28,12,3,14,16	0.26,-0.05,-0.21,-0.24,0.02,-0.46
12	31,24,18	1.72	15,12,31	1.64	33,11,12,10,3,6	-0.49,0.47,-0.14,0.26,0.02,-0.50	17,19,12	1.71	20,20,30	1.71	28,28,20,13,25,15	0.03,-0.17,0.11,-0.15,0.42,0.39
13	27,30,24	1.59	24,15,27	1.86	25,25,13,13,8,25	-0.22,-0.24,-0.24,-0.27,-0.17,0.50	25,18,22	1.44	14,25,4	1.73	12,4,19,19,15,12	-0.46,-0.16,0.24,0.24,0.27,0.50
14	9,22,25	1.55	6,22,30	1.70	18,24,25,22,22,12	-0.03,0.40,0.49,-0.47,0.47,-0.18	15,18,30	1.41	5,13,12	1.54	25,3,24,17,3,17	0.11,-0.31,-0.46,-0.37,-0.38,-0.19
15	7,30,7	1.39	10,10,15	1.61	3,18,22,25,4,22	0.33,-0.50,-0.03,0.50,-0.38,-0.24	20,5,20	1.27	17,20,29	1.53	33,8,26,3,3,33	-0.35,-0.10,-0.37,-0.09,-0.09,-0.28
16	6,17,30	1.20	9,17,6	1.61	16,21,16,25,21,12	0.39,0.32,0.34,-0.43,0.50,0.12	30,30,18	1.04	14,7,30	1.51	20,20,7,18,12,20	0.50,0.15,0.03,0.20,-0.30,0.34
17	24,30,22	0.94	9,13,25	1.53	31,32,7,32,17,17	-0.41,0.06,-0.24,-0.19,-0.02,0.35	30,17,17	0.89	9,6,13	1.51	24,4,30,24,4,13	0.49,0.50,0.25,-0.48,-0.16,0.02
18	7,14,32	0.65	30,25,9	1.47	32,32,2,18,15,15	0.50,0.18,-0.50,0.17,0.15,-0.28	9,18,30	0.58	12,28,28	1.45	32,14,18,32,12,29	-0.08,-0.18,0.25,-0.46,0.01,-0.11
19	6,6,15	0.41	15,18,18	1.47	9,15,29,30,15,30	0.40,-0.50,0.31,0.18,0.50,0.50	14,33,9	0.38	33,25,30	1.33	24,26,10,25,17,24	0.26,0.15,0.19,0.49,0.01,-0.31
20	4,13,20	0.07	30,20,15	1.45	32,32,18,25,7,29	-0.50,0.23,-0.40,0.44,-0.50,-0.50	14,29,32	0.07	5,17,32	1.40	16,11,3,32,32,11	0.23,-0.13,-0.20,0.33,0.36,-0.12
21	3,12,30	0	17,17,3	1.36	12,30,8,5,19,5	0.49,-0.36,0.15,-0.39,-0.39,0.48	15,18,11	0	6,18,30	1.20	33,33,23,2,14,23	-0.48,0.19,0.34,-0.50,-0.22,-0.38
22	9,25,26	0	18,26,30	1.33	31,20,12,20,6,6	-0.50,0.50,0.24,-0.21,-0.12,-0.38	26,30,30	0	18,13,18	1.20	15,28,12,29,31,30	-0.21,0.10,0.05,-0.36,0.50,-0.30
23	20,22,7	0	30,15,24	1.34	14,14,6,2,29,29	0.34,-0.50,-0.39,-0.05,-0.31,0.49	6,17,7	0	11,11,7	1.20	18,30,18,11,26,32	0.40,0.39,-0.29,-0.02,-0.50,-0.16
24	6,30,22	0	15,6,6	1.26	6,31,28,6,28,28	0.18,-0.09,-0.49,-0.50,-0.50,-0.50	25,18,7	0	12,25,12	1.12	4,8,18,7,6,25	0.46,-0.41,-0.48,-0.50,-0.50,-0.50

TABLE 5. Optimal feeder reconfiguration of bi-objective and tri-objective functions of SC2.

Time	Bi	Time	Bi	Time	Bi	Time	Tri	Time	Tri	Time	Tri
1	5,13,23,32,33	9	7,14,26,32,33,	17	9,14,20,24,36,	1	3,13,21,25,29,	9	9,13,18,28,31,	17	4,9,14,28,31,
2	7,9,12,25,29	10	3,11,28,31,34,	18	7,11,14,28,32,	2	2,11,12,27,30,	10	2,9,14,27,32,	18	6,9,12,27,29,
3	14,17,19,21,27	11	2,8,14,17,27,	19	7,9,17,34,37,	3	14,17,18,33,37,	11	6,13,27,29,33,	19	7,11,14,17,25,
4	6,8,14,17,24	12	5,9,13,16,28,	20	7,10,13,24,32,	4	18,27,31,33,34,	12	3,9,14,15,24,	20	4,11,12,17,28,
5	3,12,23,33,36	13	13,20,21,22,29,	21	9,13,20,28,31,	5	2,11,25,31,34,	13	3,9,17,27,34,	21	5,9,12,28,32,
6	13,20,26,31,33	14	3,9,12,28,29,	22	7,13,21,28,31,	6	2,14,15,33,37,	14	6,11,13,17,24,	22	7,9,13,27,31,
7	13,19,32,35,37	15	7,12,17,21,28,	23	5,14,17,27,33,	7	11,12,16,18,23,	15	4,10,28,30,34,	23	6,11,12,30,37,
8	3,13,17,27,35	16	4,11,13,16,24,	24	12,20,21,24,36,	8	6,10,13,25,32,	16	11,12,15,19,28,	24	5,8,28,30,34,

(DGs) and Battery Energy Storage Systems (BESS) within the power grid, incorporating network reconfiguration. The results are categorized into two cases based on the optimization objectives: Case 1 focuses on bi-objective functions—the cost of energy supplied by the grid versus energy loss cost, and Case 2 includes the additional objective of voltage deviation (VD).

In Case 1, solar DGs produce a maximum of 1.72 MW at noon (12:00) at buses 31, 24, and 18, aligned with solar irradiance availability. The minimum solar output is 0.07 MW during early morning and late evening (06:00 and 20:00 hours) at buses 17, 32, 9, 4, 13, and 20, reflecting the diurnal pattern of solar energy availability. Similarly, in Case 2, solar power peaks at 1.71 MW with DGs located at buses 17, 19, and 12, while the lowest generation of 0.07 MW is noted at 20:00 hours at buses 14, 29, and 32. Wind Turbines (WTs) generate power consistently across the period. For Case 1, the peak wind generation of 2.01 MW occurs at 01:00 and 02:00 hours at buses 26, 30, 5, and 14, 14, 25, while the lowest output of 1.26 MW is at midnight (24:00 hour) at buses 15, 6, 6. In Case 2, the maximum wind power of 2.18 MW is produced at 4:00 hours on buses 25, 22, and 9, with a minimum of 1.12 MW at midnight on buses 12, 25, and 12. The BESS units strategically charge and discharge in response to the power grid's supply and demand, ensuring a stable energy flow. Their operational patterns, as shown in Table 4, support the grid by releasing energy when there is a deficit and storing it when there is an excess. The data reflects the complex dynamics of optimizing grid performance through network reconfiguration, generation scheduling, and energy storage management. The analysis underscores the necessity of an integrated approach to grid management that prioritizes cost efficiency, reliability, and sustainability. Table 5 provides a schedule of tie switch configurations over 24 hours, detailed for both bi-objective and tri-objective optimization of SC2.

The bus numbers connected by the tie switches for each hour are listed in Table 5 for each time slot. This schedule aligns with the network reconfiguration point that was covered in the paragraphs that came before it. For example, in the bi-objective case, tie switches are scheduled to be connected at hour 1 at busses 5, 13, 23, 32, and 33. The buses at hour nine are busses 7, 14, 26, 32, and 33. This pattern illustrates the network's ability to adapt and optimize the trade-off between energy loss expenses and the overall cost of energy supplied by the grid station across a 24-hour timeframe.

Furthermore, in the case of the tri-objective scenario, the tie switches located at busses 3, 13, 21, 25, and 29 are turned on at hour 1. This adapts to maximize energy cost and loss as well as voltage variation (VD) throughout the day. The performance of solar DGs, wind turbines, and BESS units demonstrates how vital this 24-hour scheduling is to the network's resilience and adaptability, as it guarantees that the system functions effectively under a range of load circumstances and generating capabilities. The schedule considers the fluctuating power generated by renewable energy sources while helping t. The scheduling demonstrates that the network reconfiguration is dynamic and actively controlled in response to the power system's dynamic characteristics, such as the patterns of renewable energy sources' generation and the behavior of energy storage devices. As the paragraphs addressing Table 5's results make clear, this active management is essential to preserving grid stability and maximizing

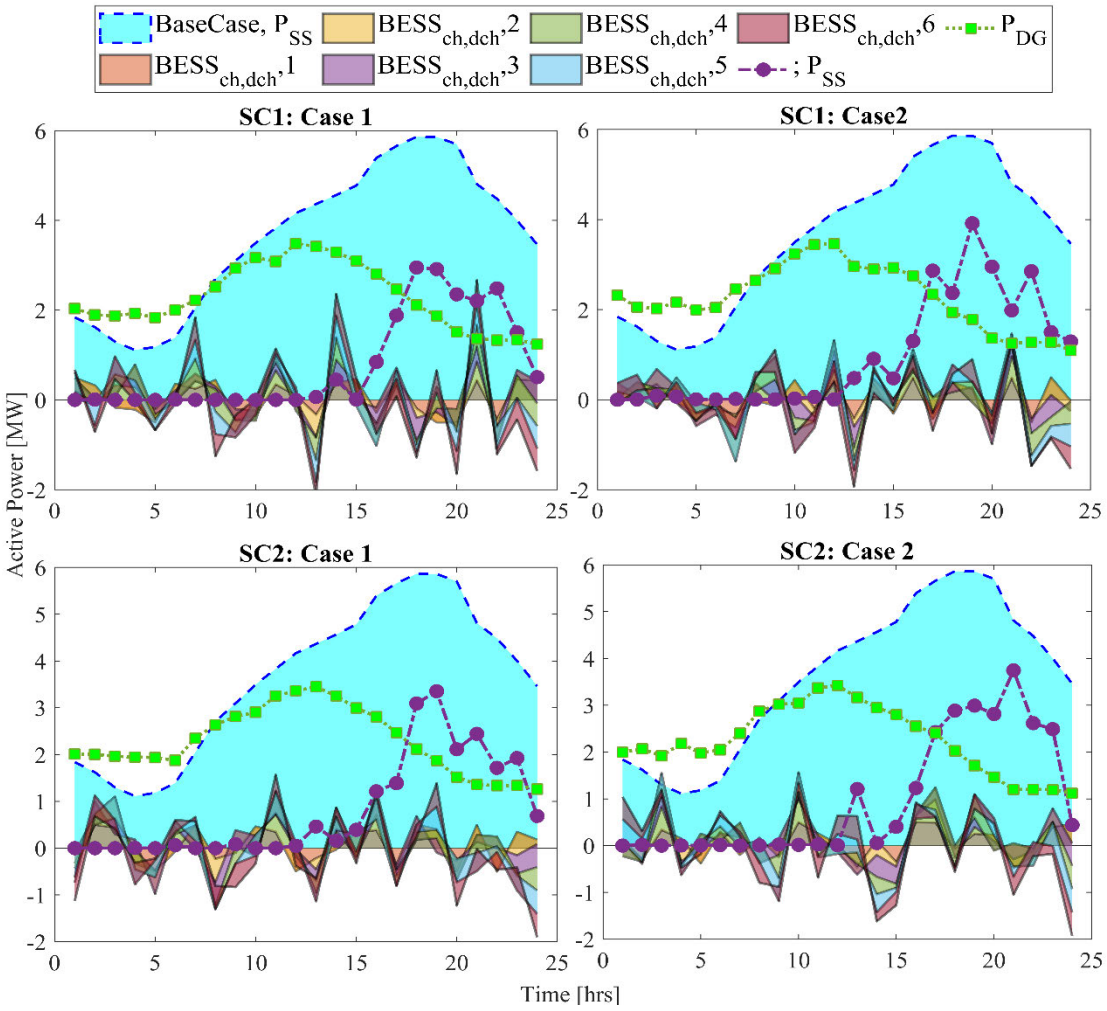

FIGURE 7. Comparison of objective functions of all the scenarios with each other.

the efficient use of dispersed generation resources and storage systems. Figure 7 compares the base case loading and the loading of all the scenarios of all the cases, DG injections, and charging and discharging of BESS devices. At low loading conditions, DG injects to balance the load demand along with charging of BESS devices; overall load due to the charging effect of BESS is increased, and hence, load demand is slightly varied and flattened. Meanwhile, power from the grid is near zero at low load conditions, increasing as demand peaks and decreases again. BESS devices are charged maximum when the load is off and discharged when the load is increased. Figure 7 also clearly shows that the proposed formulations find the best scheduling of DG and BESS devices in dynamic time-varying situations.

In Figure 7, the impacts of Distributed Generation (DG) injections and the charging and discharging of Battery Energy Storage System (BESS) devices over a 24-hour period are compared between the base-case load and the loading of all scenarios across the cases. When there are low-loading situations, DGs provide electricity to balance the load demand while also assisting with BESS device charging. Due to the charging actions of the BESS, this combined action causes a little change and flattening of the overall load, indicating an optimal supply and demand balance. At these times, almost little power is taken from the grid, demonstrating how well-distributed generators (DGs) satisfy load requirements, which rise as demand peaks and fall after that. The BESS devices are controlled strategically, charging to capacity during periods of low load and discharging during periods of high load. This cycling pattern is aptly illustrated by Figure 7, which shows how DG and BESS devices are dynamically and efficiently scheduled in response to time-varying conditions. Compared with the base case, the active power, expressed in Megawatts (MW), is shown for two situations (SC1 and SC2) over two instances. The basic scenario is intended to show how well the power system functions without solar, wind, or BESS integration. Furthermore, Figure 7's BESS charging and discharging lines illustrate the many tactics used all day to control power levels successfully. These tactics outline how BESS might reduce power demand variations

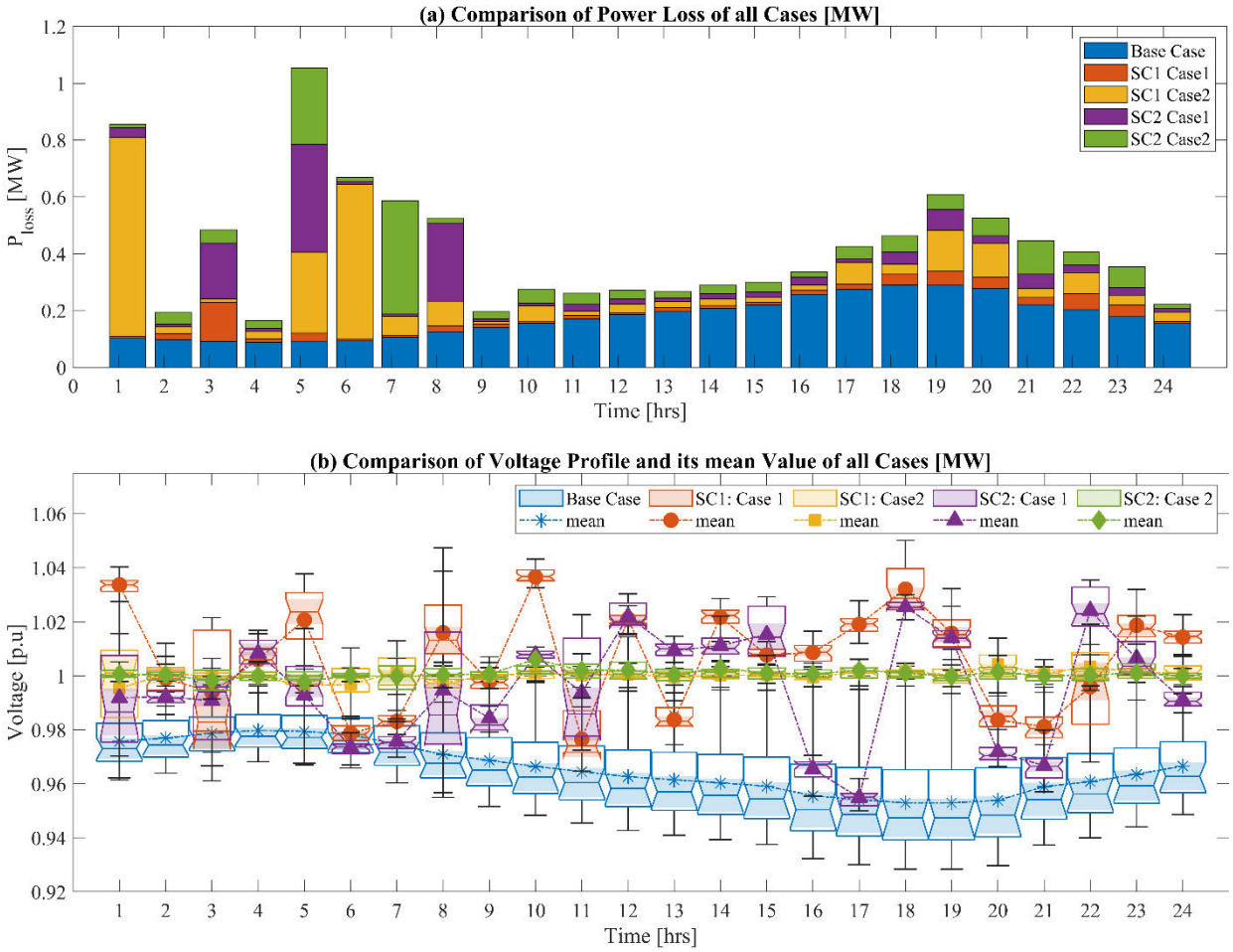

FIGURE 8. Box plot and mean of (a) Active Power Loss and (b) Voltage Profile with and without ONR of the entire time horizon.

and create a more dependable and effective energy system. The power profile of the grid is significantly impacted by the addition of DGs and different BESS techniques, as seen by smoother curves and lower peak demands. In BESS and DG integrated scenarios, BESS energy resource management results in constant power levels, flattening peaks, and filling valleys throughout the day. As essential components of contemporary power networks, this emphasizes the strategic application of DG and BESS and suggests increased grid resilience and efficiency. Additionally, Figure 8 displays the power loss and box plot of the voltage profile across the whole horizon for each studied situation.

Figure 8 (a) gives a detailed comparison across various scenarios (SC1 and SC2) and cases (Base Case, Case 1, and Case 2). It displays the power loss in megawatts (MW) across a 24-hour period. The base case typically shows the highest power loss at various times, indicating inefficiencies operating without integrating solar and wind DGs or BESS. SC1 and SC2 in both case 1 and case 2 exhibit lower losses. In contrast, with SC2, Case 2 shows the most significant reduction of power losses, suggesting the optimal usage of DGs and BESS in that scenario. Figure 8 (b) compares voltage profiles in the different scenarios. It plots voltage per unit (p.u.) over 24 hours, with markers indicating mean values. The base case shows more volatility and generally lower voltage levels. Voltage stability improves with the introduction of DG and BESS into the power system, as evidenced by the narrower boxplots and higher mean voltage levels in SC1 and SC2 compared to the base case. The SC2 in case 2 shows the almost unity voltage (p.u) throughout the time span validation of the optimal network configurations and integration of DGs and BESS. These graphical representations underscore the benefits of integrating DG and BESS into power systems for reducing losses and maintaining voltage stability. The comparison of BCS solution of the entire time horizon of Scenario 1 (without network reconfiguration) and Scenario 2 of cases 1 and 2 (simultaneously optimization of bi and tri-objective functions) is presented in Table 6.

Simulation of results shown in Table 6 compares the cost of energy supplied versus the cost of energy loss for case 1 and adds the Voltage Deviation (VD) objective for case 2. Table 6 details the most frequently selected sites for photovoltaic (PV) solar panels, wind turbines (WT), and Battery Energy Storage Systems (BESS), along with their

TABLE 6. Comparison of Simulation results of Base Case, Case 1, and Case 2 of both the scenarios.

Quantity	Base Case	SC1		SC2	
		Case 1	Case 2	Case 1	Case 2
$site_{PV}$	--	7, 14, 30	30, 30, 25,	6, 30, 7,	15, 18, 30,
$site_{WT}$	--	30, 30, 25,	3, 18, 25,	15, 10, 6,	12, 25, 30,
$site_{BESS}$	--	11, 32, 12, 8, 5, 2	31, 13, 17, 2, 3, 8,	3, 32, 3, 25, 4, 12,	12, 8, 18, 17, 32, 24,
$size_{PV}$ [MWh/day]	--	4.973, 4.864, 4.743	4.765, 4.787, 4.800,	4.974, 4.961, 4.697,	4.647, 4.654, 4.663,
$size_{WT}$ [MWh/day]	--	13.499, 13.459, 13.326	13.270, 13.778, 13.224	13.549, 13.448, 13.201	13.197, 13.586, 13.351
P_{ch} [MWh/day]	--	4.979, 3.605, 2.954, 4.016, 3.488, 3.243	3.770, 3.499, 3.510, 3.159, 2.469, 3.128	4.872, 4.524, 3.655, 3.258, 3.383, 4.008	4.324, 3.530, 2.523, 3.315, 3.097, 2.558
P_{dch} [MWh/day]	--	-3.903, -2.784, -3.807, -4.713, -4.458, -4.259	-3.487, -3.002, -3.794, -4.181, -3.632, -4.109	-3.684, -4.419, -4.584, -4.272, -4.372, -4.471	-2.702, -2.462, -3.191, -4.308, -4.140, -3.699
C_{SS} [$/day]	2.81E+06	714168.4673	893447.3936	743910.6082	901173.3672
C_{DG} [$/day]	--	702104.1886	698554.3561	701846.2589	691065.3588
C_{BESS} [$/day]	--	167461.1503	155434.0182	180613.5681	143515.1411
CEL [$/day]	3.39E+05	48878.3698	199115.583	107902.5679	123803.1967
VD [p.u]	29.09708	6.6457	0.39611	8.1575	0.19919
P_{SS} [MW/day]	86.72709	18.1993	23.1802	19.1499	23.4118
P_{loss} [MW/day]	4.214963	0.607232995	2.473682169	1.340511145	1.538050189

respective sizes in MWh/day and costs associated with each component of the system (C_DG) for distributed generation costs, C_BESS for battery storage costs, and CEL for energy loss costs). In Scenario 1 (SC1), solar panels are most often placed at sites 7, 14, and 30 for case 1, and at sites 30, 30, and 25 for case 2, while in Scenario 2 (SC2), they are placed at sites 6, 30, and 7 for case 1, and 15, 18, and 30 for case 2. Wind turbines follow a similar pattern of placement across both scenarios and cases. The most frequent sites for BESS vary more significantly, with six different sites chosen for each scenario and case. The PV and WT sizes and the BESS's charging and discharging capacity are given to show how much energy each system provides or uses daily. Table 6 also shows the voltage variation (VD), power supplied by the mainstream substation, and the daily costs of energy loss (CEL), distributed generation (CDG), and battery storage (CBESS). Furthermore, the efficiency of the grid's power distribution is indicated by the reported power loss (P_loss). A thorough overview of the cost-effectiveness and operational efficiency of the various energy generating and storage systems under the multiple optimization scenarios and instances is provided in Table 6. It examines the effects of different optimization techniques while accounting for the interactions between energy production, storage, and the physical layout of the grid.

VI. CONCLUSION

This paper introduces a thorough algorithm for improving the efficiency of power distribution networks. It achieves this by integrating distributed resources, which include DGs and BESs, with efficient network reconfiguration. The study employs a cutting-edge multi-objective optimization method, i.e., an Improved Bidirectional Coevolutionary (I-BiCo) algorithm, to substantially decrease energy costs, power losses, and voltage variations. The combination of solar PV and wind DGs, BESs, and optimal power flow can dramatically improve the distributed networks' flexibility, dependability, and sustainability while plummeting the intrinsic volatility of renewable energy sources. Through several simulations and comparisons, the research validates the algorithm's effectiveness. It establishes that the proposed method surpasses the current Multi-Objective Evolutionary Algorithms (MOEAs) regarding convergence, variety, and solution quality. This paper yields considerable developments in the optimization of power distribution by offering strategies and recommendations for evolving effective and eco-friendly power systems in a continually varying energy environment. This research underlines the significance of BESS in refining grid stability and reducing power variations, particularly when integrating unpredictable renewable energy sources. Tshis paper presents a complex ONR approach to optimize the utilization of renewable energy, minimizing costs and inefficiencies and incorporating distributed generators with battery energy storage systems. The study focuses on the development and advantages of distributed resource allocation and multi-period optimum network reconfiguration, encompassing technical and economic goals. This study not only underlines the importance of comprehensive methodologies for improving the efficiency of power distribution networks but also provides valuable insights and ideas that will contribute to the future advancement of energy system management and sustainability.

ACKNOWLEDGMENT

This work was supported by the Deanship of Scientific Research at Northern Border University, Arar, Saudia Arabia, under Project ''NBU-FFR-2024-2448-05''.

REFERENCES

[1] *IEEE Guide for Design, Operation, and Integration of Distributed Resource Island Systems With Electric Power Systems*, IEEE Standard 1547.4-2011, 2011, pp. 1–54, doi: 10.1109/IEEESTD.2011.5960751.

[2] I. Ben Hamida, S. B. Salah, F. Msahli, and M. F. Mimouni, ''Optimal network reconfiguration and renewable DG integration considering time sequence variation in load and DGs,'' *Renew. Energy*, vol. 121, pp. 66–80, Jun. 2018, doi: 10.1016/j.renene.2017.12.106.

[3] M. E. Baran and F. F. Wu, ''Network reconfiguration in distribution systems for loss reduction and load balancing,'' (in English), *IEEE Trans. Power Del.*, vol. 4, no. 2, pp. 1401–1407, Apr. 1989, doi: 10.1109/61.25627.

[4] M. A. Samman, H. Mokhlis, N. N. Mansor, H. Mohamad, H. Suyono, and N. M. Sapari, ''Fast optimal network reconfiguration with guided initialization based on a simplified network approach,'' *IEEE Access*, vol. 8, pp. 11948–11963, 2020, doi: 10.1109/ACCESS.2020.2964848.

[5] A. Merlin and H. Back, ''Search for a minimal-loss operating spanning tree configuration in an urban power distribution system,'' in *Proc. 5th Power Syst. Comput. Conf. (PSCC)*, 1975, p. 1.

[6] M. Abdelaziz, ''Distribution network reconfiguration using a genetic algorithm with varying population size,'' *Electr. Power Syst. Res.*, vol. 142, pp. 9–11, Jan. 2017, doi: 10.1016/j.epsr.2016.08.026.

[7] D.-L. Duan, X.-D. Ling, X.-Y. Wu, and B. Zhong, ''Reconfiguration of distribution network for loss reduction and reliability improvement based on an enhanced genetic algorithm,'' *Int. J. Electr. Power Energy Syst.*, vol. 64, pp. 88–95, Jan. 2015, doi: 10.1016/j.ijepes.2014.07.036.

[8] T. Niknam, A. K. Fard, and A. Seifi, ''Distribution feeder reconfiguration considering fuel cell/wind/photovoltaic power plants,'' *Renew. Energy*, vol. 37, no. 1, pp. 213–225, Jan. 2012, doi: 10.1016/j.renene.2011.06.017.

[9] S. Teimourzadeh and K. Zare, ''Application of binary group search optimization to distribution network reconfiguration,'' *Int. J. Electr. Power Energy Syst.*, vol. 62, pp. 461–468, Nov. 2014, doi: 10.1016/j.ijepes.2014.04.064.

[10] A. Asrari, S. Lotfifard, and M. S. Payam, ''Pareto dominance-based multiobjective optimization method for distribution network reconfiguration,'' *IEEE Trans. Smart Grid*, vol. 7, no. 3, pp. 1401–1410, May 2016, doi: 10.1109/TSG.2015.2468683.

[11] R. M. Vitorino, H. M. Jorge, and L. P. Neves, ''Multi-objective optimization using NSGA-II for power distribution system reconfiguration,'' *Int. Trans. Electr. Energy Syst.*, vol. 25, no. 1, pp. 38–53, Jan. 2015, doi: 10.1002/etep.1819.

[12] F. R. Alonso, D. Q. Oliveira, and A. C. Zambroni de Souza, ''Artificial immune systems optimization approach for multiobjective distribution system reconfiguration,'' *IEEE Trans. Power Syst.*, vol. 30, no. 2, pp. 840–847, Mar. 2015, doi: 10.1109/TPWRS.2014.2330628.

[13] W. El-Khattam and M. M. A. Salama, ''Distributed generation technologies, definitions and benefits,'' *Electr. Power Syst. Res.*, vol. 71, no. 2, pp. 119–128, Oct. 2004, doi: 10.1016/j.epsr.2004.01.006.

[14] M. Thirunavukkarasu, Y. Sawle, and H. Lala, ''A comprehensive review on optimization of hybrid renewable energy systems using various optimization techniques,'' *Renew. Sustain. Energy Rev.*, vol. 176, Apr. 2023, Art. no. 113192, doi: 10.1016/j.rser.2023.113192.

[15] K. Bano, G. Abbas, M. Hatatah, E. Touti, A. Emara, and P. Mercorelli, ''Phase shift APOD and POD control technique in multi-level inverters to mitigate total harmonic distortion,'' *Mathematics*, vol. 12, no. 5, p. 656, 2024, doi: 10.3390/math12050656.

[16] D. Q. Hung and N. Mithulananthan, ''Loss reduction and loadability enhancement with DG: A dual-index analytical approach,'' *Appl. Energy*, vol. 115, pp. 233–241, Feb. 2014, doi: 10.1016/j.apenergy.2013.11.010.

[17] G. Abbas, Z. Wu, and A. Ali, ''Multi-objective multi-period optimal site and size of distributed generation along with network reconfiguration,'' *IET Renew. Power Gener.*, pp. 1–27, 2024, doi: 10.1049/rpg2.12949.

[18] Y. M. Atwa, E. F. El-Saadany, M. M. A. Salama, and R. Seethapathy, ''Optimal renewable resources mix for distribution system energy loss minimization,'' *IEEE Trans. Power Syst.*, vol. 25, no. 1, pp. 360–370, Feb. 2010, doi: 10.1109/TPWRS.2009.2030276.

[19] A. El-Fergany, ''Optimal allocation of multi-type distributed generators using backtracking search optimization algorithm,'' *Int. J. Electr. Power Energy Syst.*, vol. 64, pp. 1197–1205, Jan. 2015, doi: 10.1016/j.ijepes.2014.09.020.

[20] S. R. Gampa and D. Das, ''Optimum placement and sizing of DGs considering average hourly variations of load,'' *Int. J. Electr. Power Energy Syst.*, vol. 66, pp. 25–40, Mar. 2015, doi: 10.1016/j.ijepes.2014.10.047.

[21] A. Ali, G. Abbas, M. U. Keerio, S. Mirsaeidi, S. Alshahr, and A. Alshahir, ''Pareto front-based multiobjective optimization of distributed generation considering the effect of voltage-dependent nonlinear load models,'' *IEEE Access*, vol. 11, pp. 12195–12217, 2023, doi: 10.1109/ACCESS.2023.3242546.

[22] A. Ali, G. Abbas, M. U. Keerio, S. Mirsaeidi, S. Alshahr, and A. Alshahir, ''Multi-objective optimal siting and sizing of distributed generators and shunt capacitors considering the effect of voltage-dependent nonlinear load models,'' *IEEE Access*, vol. 11, pp. 21465–21487, 2023, doi: 10.1109/ACCESS.2023.3250760.

[23] K. Vinothkumar and M. P. Selvan, ''Fuzzy embedded genetic algorithm method for distributed generation planning,'' *Electr. Power Compon. Syst.*, vol. 39, no. 4, pp. 346–366, Feb. 2011, doi: 10.1080/15325008.2010.528533.

[24] G. Abbas, M. Hatatah, A. Ali, E. Touti, A. Alshahir, and A. M. Elrashidi, ''A novel energy proficient computing framework for green computing using sustainable energy sources,'' *IEEE Access*, vol. 11, pp. 126542–126554, 2023, doi: 10.1109/access.2023.3331987.

[25] W. Sheng, K.-Y. Liu, Y. Liu, X. Meng, and Y. Li, ''Optimal placement and sizing of distributed generation via an improved nondominated sorting genetic algorithm II,'' *IEEE Trans. Power Del.*, vol. 30, no. 2, pp. 569–578, Apr. 2015, doi: 10.1109/TPWRD.2014.2325938.

[26] K. Nekooei, M. M. Farsangi, H. Nezamabadi-Pour, and K. Y. Lee, ''An improved multi-objective harmony search for optimal placement of DGs in distribution systems,'' *IEEE Trans. Smart Grid*, vol. 4, no. 1, pp. 557–567, Mar. 2013, doi: 10.1109/TSG.2012.2237420.

[27] A. Ali, G. Abbas, M. U. Keerio, M. A. Koondhar, K. Chandni, and S. Mirsaeidi, ''Solution of constrained mixed-integer multi-objective optimal power flow problem considering the hybrid multi-objective evolutionary algorithm,'' *IET Gener., Transmiss. Distrib.*, vol. 17, no. 1, pp. 66–90, Jan. 2023, doi: 10.1049/gtd2.12664.

[28] T. Tran The, B.-H. Truong, K. Dang Tuan, and D. Vo Ngoc, ''A nondominated sorting stochastic fractal search algorithm for multiobjective distribution network reconfiguration with distributed generations,'' *Math. Problems Eng.*, vol. 2021, pp. 1–20, Feb. 2021, doi: 10.1155/2021/6638559.

[29] G. J. S. Rosseti, E. J. de Oliveira, L. W. de Oliveira, I. C. Silva, and W. Peres, ''Optimal allocation of distributed generation with reconfiguration in electric distribution systems,'' *Electr. Power Syst. Res.*, vol. 103, pp. 178–183, Oct. 2013, doi: 10.1016/j.epsr.2013.05.017.

[30] A. Mohamed Imran, M. Kowsalya, and D. P. Kothari, ''A novel integration technique for optimal network reconfiguration and distributed generation placement in power distribution networks,'' *Int. J. Electr. Power Energy Syst.*, vol. 63, pp. 461–472, Dec. 2014, doi: 10.1016/j.ijepes.2014.06.011.

[31] A. Bayat, A. Bagheri, and R. Noroozian, ''Optimal siting and sizing of distributed generation accompanied by reconfiguration of distribution networks for maximum loss reduction by using a new UVDA-based heuristic method,'' *Int. J. Electr. Power Energy Syst.*, vol. 77, pp. 360–371, May 2016, doi: 10.1016/j.ijepes.2015.11.039.

[32] T. H. B. Huy, T. V. Tran, D. Ngoc Vo, and H. T. T. Nguyen, ''An improved metaheuristic method for simultaneous network reconfiguration and distributed generation allocation,'' *Alexandria Eng. J.*, vol. 61, no. 10, pp. 8069–8088, Oct. 2022, doi: 10.1016/j.aej.2022.01.056.

[33] A. M. Shaheen, A. M. Elsayed, R. A. El-Sehiemy, and A. Y. Abdelaziz, ''Equilibrium optimization algorithm for network reconfiguration and distributed generation allocation in power systems,'' *Appl. Soft Comput.*, vol. 98, Jan. 2021, Art. no. 106867, doi: 10.1016/j.asoc.2020.106867.

[34] H. Bagheri Tolabi, M. H. Ali, and M. Rizwan, ''Simultaneous reconfiguration, optimal placement of DSTATCOM, and photovoltaic array in a distribution system based on fuzzy-ACO approach,'' *IEEE Trans. Sustain. Energy*, vol. 6, no. 1, pp. 210–218, Jan. 2015, doi: 10.1109/TSTE.2014.2364230.

[35] M. Esmaeili, M. Sedighizadeh, and M. Esmaili, ''Multi-objective optimal reconfiguration and DG (distributed generation) power allocation in distribution networks using big bang-big crunch algorithm considering load uncertainty,'' *Energy*, vol. 103, pp. 86–99, May 2016, doi: 10.1016/j.energy.2016.02.152.

[36] N. Kanwar, N. Gupta, K. R. Niazi, A. Swarnkar, and R. C. Bansal, "Simultaneous allocation of distributed energy resource using improved particle swarm optimization," *Appl. Energy*, vol. 185, pp. 1684–1693, Jan. 2017, doi: 10.1016/j.apenergy.2016.01.093.
[37] E. M. Ahmed, S. Rakočević, M. Ćalasan, Z. M. Ali, H. M. Hasanien, R. A. Turky, and S. H. E. A. Aleem, "BONMIN solver-based coordination of distributed FACTS compensators and distributed generation units in modern distribution networks," *Ain Shams Eng. J.*, vol. 13, no. 4, Jun. 2022, Art. no. 101664, doi: 10.1016/j.asej.2021.101664.
[38] Y. Li, B. Feng, B. Wang, and S. Sun, "Joint planning of distributed generations and energy storage in active distribution networks: A bi-level programming approach," *Energy*, vol. 245, Apr. 2022, Art. no. 123226, doi: 10.1016/j.energy.2022.123226.
[39] M. M. Ansari, C. Guo, M. S. Shaikh, N. Chopra, I. Haq, and L. Shen, "Planning for distribution system with grey wolf optimization method," *J. Electr. Eng. Technol.*, vol. 15, no. 4, pp. 1485–1499, Jul. 2020, doi: 10.1007/s42835-020-00419-4.
[40] A. Eid, S. Kamel, A. Korashy, and T. Khurshaid, "An enhanced artificial ecosystem-based optimization for optimal allocation of multiple distributed generations," *IEEE Access*, vol. 8, pp. 178493–178513, 2020, doi: 10.1109/ACCESS.2020.3027654.
[41] E. A. Almabsout, R. A. El-Sehiemy, O. N. U. An, and O. Bayat, "A hybrid local search-genetic algorithm for simultaneous placement of DG units and shunt capacitors in radial distribution systems," *IEEE Access*, vol. 8, pp. 54465–54481, 2020, doi: 10.1109/ACCESS.2020.2981406.
[42] A. Eid, "Cost-based analysis and optimization of distributed generations and shunt capacitors incorporated into distribution systems with nonlinear demand modeling," *Expert Syst. Appl.*, vol. 198, Jul. 2022, Art. no. 116844, doi: 10.1016/j.eswa.2022.116844.
[43] K. Balu and V. Mukherjee, "Siting and sizing of distributed generation and shunt capacitor banks in radial distribution system using constriction factor particle swarm optimization," *Electr. Power Compon. Syst.*, vol. 48, nos. 6–7, pp. 697–710, Apr. 2020.
[44] A. K. Barnwal, L. K. Yadav, and M. K. Verma, "A multi-objective approach for voltage stability enhancement and loss reduction under PQV and P buses through reconfiguration and distributed generation allocation," *IEEE Access*, vol. 10, pp. 16609–16623, 2022.
[45] A. Ali, G. Abbas, M. U. Keerio, E. Touti, Z. Ahmed, O. Alsalman, and Y.-S. Kim, "A bi-level techno-economic optimal reactive power dispatch considering wind and solar power integration," *IEEE Access*, vol. 11, pp. 62799–62819, 2023, doi: 10.1109/ACCESS.2023.3286930. https://doi.org/10.1109/ACCESS.2023.3286930.
[46] C. Venkatesan, R. Kannadasan, M. H. Alsharif, M.-K. Kim, and J. Nebhen, "A novel multiobjective hybrid technique for siting and sizing of distributed generation and capacitor banks in radial distribution systems," *Sustainability*, vol. 13, no. 6, p. 3308, Mar. 2021.
[47] M. J. Hadidian-Moghaddam, S. Arabi-Nowdeh, M. Bigdeli, and D. Azizian, "A multi-objective optimal sizing and siting of distributed generation using ant lion optimization technique," *Ain Shams Eng. J.*, vol. 9, no. 4, pp. 2101–2109, Dec. 2018.
[48] B. Mukhopadhyay and D. Das, "Multi-objective dynamic and static reconfiguration with optimized allocation of PV-DG and battery energy storage system," *Renew. Sustain. Energy Rev.*, vol. 124, May 2020, Art. no. 109777, doi: 10.1016/j.rser.2020.109777.
[49] A. Ali, A. Shah, M. U. Keerio, N. H. Mugheri, G. Abbas, E. Touti, M. Hatatah, A. Yousef, and M. Bouzguenda, "Multi-objective security constrained unit commitment via hybrid evolutionary algorithms," *IEEE Access*, vol. 12, pp. 6698–6718, 2024, doi: 10.1109/access.2024.3351710.
[50] M. G. Hemeida, S. Alkhalaf, A.-A.-A. Mohamed, A. A. Ibrahim, and T. Senjyu, "Distributed generators optimization based on multi-objective functions using manta rays foraging optimization algorithm (MRFO)," *Energies*, vol. 13, no. 15, p. 3847, Jul. 2020, doi: 10.3390/en13153847.
[51] A. Noori, Y. Zhang, N. Nouri, and M. Hajivand, "Multi-objective optimal placement and sizing of distribution static compensator in radial distribution networks with variable residential, commercial and industrial demands considering reliability," *IEEE Access*, vol. 9, pp. 46911–46926, 2021, doi: 10.1109/ACCESS.2021.3065883.
[52] M. Kefayat, A. L. Ara, and S. A. N. Niaki, "A hybrid of ant colony optimization and artificial bee colony algorithm for probabilistic optimal placement and sizing of distributed energy resources," *Energy Convers. Manage.*, vol. 92, pp. 149–161, Mar. 2015, doi: 10.1016/j.enconman.2014.12.037.
[53] R. Jing, X. Zhu, Z. Zhu, W. Wang, C. Meng, N. Shah, N. Li, and Y. Zhao, "A multi-objective optimization and multi-criteria evaluation integrated framework for distributed energy system optimal planning," *Energy Convers. Manage.*, vol. 166, pp. 445–462, Jun. 2018.
[54] S. Zeynali, N. Rostami, and M. R. Feyzi, "Multi-objective optimal short-term planning of renewable distributed generations and capacitor banks in power system considering different uncertainties including plug-in electric vehicles," *Int. J. Electr. Power Energy Syst.*, vol. 119, Jul. 2020, Art. no. 105885.
[55] H. Lotfi, "Optimal sizing of distributed generation units and shunt capacitors in the distribution system considering uncertainty resources by the modified evolutionary algorithm," *J. Ambient Intell. Humanized Comput.*, vol. 13, no. 10, pp. 4739–4758, Oct. 2022, doi: 10.1007/s12652-021-03194-w.
[56] I. Soesanti and R. Syahputra, "Multiobjective ant lion optimization for performance improvement of modern distribution network," *IEEE Access*, vol. 10, pp. 12753–12773, 2022.
[57] S. A. S. Mustaffa, I. Musirin, M. K. M. Zamani, and M. M. Othman, "Pareto optimal approach in multi-objective chaotic mutation immune evolutionary programming (MOCMIEP) for optimal distributed generation photovoltaic (DGPV) integration in power system," *Ain Shams Eng. J.*, vol. 10, no. 4, pp. 745–754, Dec. 2019.
[58] M. I. Akbar, S. A. A. Kazmi, O. Alrumayh, Z. A. Khan, A. Altamimi, and M. M. Malik, "A novel hybrid optimization-based algorithm for the single and multi-objective achievement with optimal DG allocations in distribution networks," *IEEE Access*, vol. 10, pp. 25669–25687, 2022, doi: 10.1109/ACCESS.2022.3155484.
[59] B. Ahmadi, O. Ceylan, and A. Ozdemir, "A multi-objective optimization evaluation framework for integration of distributed energy resources," *J. Energy Storage*, vol. 41, Sep. 2021, Art. no. 103005, doi: 10.1016/j.est.2021.103005.
[60] P. P. Biswas, R. Mallipeddi, P. N. Suganthan, and G. A. J. Amaratunga, "A multiobjective approach for optimal placement and sizing of distributed generators and capacitors in distribution network," *Appl. Soft Comput.*, vol. 60, pp. 268–280, Nov. 2017.
[61] A. Ali, M. U. Keerio, and J. A. Laghari, "Optimal site and size of distributed generation allocation in radial distribution network using multi-objective optimization," *J. Mod. Power Syst. Clean Energy*, vol. 9, no. 2, pp. 404–415, Mar. 2021, doi: 10.35833/MPCE.2019.000055.
[62] A. Selim, S. Kamel, F. Jurado, J. A. P. Lopes, and M. Matos, "Optimal setting of PV and battery energy storage in radial distribution systems using multi-objective criteria with fuzzy logic decision-making," *IET Gener., Transmiss. Distrib.*, vol. 15, no. 1, pp. 135–148, Jan. 2021, doi: 10.1049/gtd2.12019.
[63] K. Deb, A. Pratap, S. Agarwal, and T. Meyarivan, "A fast and elitist multiobjective genetic algorithm: NSGA-II," *IEEE Trans. Evol. Comput.*, vol. 6, no. 2, pp. 182–197, Apr. 2002, doi: 10.1109/4235.996017.
[64] P. Lata and S. Vadhera, "Reliability improvement of radial distribution system by optimal placement and sizing of energy storage system using TLBO," *J. Energy Storage*, vol. 30, Aug. 2020, Art. no. 101492, doi: 10.1016/j.est.2020.101492.
[65] T. Adefarati and R. C. Bansal, "Reliability assessment of distribution system with the integration of renewable distributed generation," *Appl. Energy*, vol. 185, pp. 158–171, Jan. 2017, doi: 10.1016/j.apenergy.2016.10.087.
[66] Z.-Z. Liu, B.-C. Wang, and K. Tang, "Handling constrained multiobjective optimization problems via bidirectional coevolution," *IEEE Trans. Cybern.*, vol. 52, no. 10, pp. 10163–10176, Oct. 2022, doi: 10.1109/TCYB.2021.3056176.
[67] B. Ahmadi, O. Ceylan, A. Ozdemir, and M. Fotuhi-Firuzabad, "A multi-objective framework for distributed energy resources planning and storage management," *Appl. Energy*, vol. 314, May 2022, Art. no. 118887, doi: 10.1016/j.apenergy.2022.118887.
[68] N.-M. Zografou-Barredo, C. Patsios, I. Sarantakos, P. Davison, S. L. Walker, and P. C. Taylor, "MicroGrid resilience-oriented scheduling: A robust MISOCP model," *IEEE Trans. Smart Grid*, vol. 12, no. 3, pp. 1867–1879, May 2021, doi: 10.1109/TSG.2020.3039713.
[69] Y. Tian, R. Cheng, X. Zhang, and Y. Jin, "PlatEMO: A MATLAB platform for evolutionary multi-objective optimization [educational forum]," *IEEE Comput. Intell. Mag.*, vol. 12, no. 4, pp. 73–87, Nov. 2017, doi: 10.1109/MCI.2017.2742868.
[70] F. Ming, W. Gong, and L. Gao, "Adaptive auxiliary task selection for multitasking-assisted constrained multi-objective optimization [feature]," *IEEE Comput. Intell. Mag.*, vol. 18, no. 2, pp. 18–30, May 2023, doi: 10.1109/MCI.2023.3245719.
[71] Y. Tian, T. Zhang, J. Xiao, X. Zhang, and Y. Jin, "A coevolutionary framework for constrained multiobjective optimization problems," *IEEE Trans. Evol. Comput.*, vol. 25, no. 1, pp. 102–116, Feb. 2021.

[72] E. Davoodi, E. Babaei, and B. Mohammadi-ivatloo, "An efficient covexified SDP model for multi-objective optimal power flow," *Int. J. Electr. Power Energy Syst.*, vol. 102, pp. 254–264, Nov. 2018, doi: 10.1016/j.ijepes.2018.04.034.

ASIF ALI is currently pursuing the Ph.D. degree with Shandong University, China. His research interests include power system optimization, grid-connected and islanded operation of distributed generation and smart grids, electric vehicles, and battery systems.

ZHIZHEN LIU is currently with the School of Electrical Engineering, Shandong University, China. His research interests include the optimization design and operation analysis of electrical equipment, power quality research, and wireless power transmission research.

AAMIR ALI received the B.E., M.E., and Ph.D. degrees in electrical engineering from QUEST, Nawabshah, Pakistan. He is currently an Assistant Professor with the Department of Electrical Engineering, Quaid-e-Awam University of Engineering Science and Technology (QUEST), Nawabshah, Sindh, Pakistan. His research interests include power system optimization, grid-connected and islanded operation of distributed generation, smart grids, and multi-objective evolutionary algorithms.

GHULAM ABBAS received the B.Eng. degree in electrical engineering from QUEST, Nawabshah, Pakistan, in 2017, and the M.Eng. degree in electrical engineering from Southeast University, Nanjing, China, in 2019, where he is currently pursuing the Ph.D. degree in electrical engineering. His research interests include distributed generation integration, planning, and optimization.

EZZEDDINE TOUTI received the B.S. degree in electrical engineering from the Higher National College of Engineers of Tunis, Tunisia, in 1997, the master's degree in electrical engineering from the National College of Engineers of Tunis, Tunisia, in 2005, and the joint Ph.D. degree in induction generators wind turbine, power quality and electric drives from the National College of Engineers of Monastir, Tunisia, and Artois University, France, in 2013. In 2005, he joined the Laboratory of Industrial Systems Engineering and Renewable Energies (LISIER), University of Tunis, Tunisia, as a Research Faculty Member. He is currently an Associate Professor with the College of Engineering, Northern Border University. His research interests include renewable energy, smart grids, electric vehicles, power electronics, and the control of electrical systems.

WALEED NURELDEEN is currently an Assistant Professor with the Department of General Subjects, College of Engineering, University of Business and Technology, Jeddah, Saudi Arabia.